both loxoprofen and loxoprofen-OH showed weak activity for hemolysis (Fig. 3B). Loxoprofen showed lower permeabilization activity than loxoprofen-OH on the hemolysis assay (Fig. 3B).

The results shown in Fig. 3 suggest that the low direct cytotoxicity of loxoprofen and loxoprofen-OH on gastric mucosal cells is due to their low membrane permeabilizing effects.

Cytotoxic Effects of Loxoprofen and Loxoprofen-OH on Gastric Cancer Cells In addition to their anti-inflammatory effects, recent epidemiological studies have revealed that prolonged NSAID use reduces the risk of cancer, while preclinical and clinical studies have indicated that some NSAIDs are effective in the treatment and prevention of cancer.[35] The anti-tumorigenic activity of NSAIDs is believed to involve various mechanisms, including induction of apoptosis.[36,37] Thus, it is important to examine the apoptosis-inducing ability of loxoprofen in cancer cells and we here used cultured AGS cells for this purpose.

As shown in Fig. 4A, each NSAID induced apoptosis in a dose dependent manner in AGS cells and loxoprofen and loxoprofen-OH showed less activity for inducing apoptosis than indomethacin and celecoxib. We confirmed that cell death observed in Fig. 4A is mediated by apoptosis, because it was accompanied by apoptotic DNA fragmentation and apoptotic chromatin condensation (Figs. 4B, C). Comparing to data in primary culture of gastric mucosal cells (Fig. 2), loxoprofen and loxoprofen-OH induced apoptosis more potently in AGS cells. The ED_{70} values of NSAIDs for apoptosis (concentrations of NSAIDs required for 70% cell viability by apoptosis) of loxoprofen and loxoprofen-OH were lower in AGS cells than in primary culture of gastric mucosal cells (Table 1). On the other hand, the ED_{70} values for apoptosis of indomethacin and celecoxib were nearly indistinguishable between AGS cells and primary culture of gastric mucosal cells (Table 1). Although the underlying mechanism is unknown at present, this character of loxoprofen and loxoprofen-OH may be clinically beneficial for their application as anti-tumor drugs.

We also examined the effect of NSAIDs on the COX activity in cultured AGS cells. As shown in Fig. 4D, each of all NSAIDs tested decreased the amount of PGE_2 in the culture medium, in other words, inhibited COX activity in a dose dependent manner.

In summary, we show here that loxoprofen and loxoprofen-OH have a very low level of direct cytotoxicity on gastric mucosal cells *in vitro*. As described above, it is well known that loxoprofen is clinically safe on gastric mucosa compared to other NSAIDs such as indomethacin.[25,26] We propose here that the low direct cytotoxicity of loxoprofen make it less harmful on the gastric mucosa for clinical use.

As described above, we have suggested that both COX inhibition (decrease in gastric level of PGE_2) and gastric mucosal cell death are required for the formation of NSAID-induced gastric lesions *in vivo* (Fig. 5).[20,24] Based on this idea, either NSAIDs without decreasing gastric level of PGE_2 or NSAIDs with lower cytotoxic effect should be safe NSAIDs on gastric mucosa. In other words, NSAIDs that have high cytotoxic effect on gastric mucosa and high ability to inhibit COX-1 expressed in gastric mucosa should have high risk for formation of gastric lesions. Indomethacin belongs to this type of NSAIDs and has relatively high risk for formation of gastric lesions clinically. Selective COX-2 inhibitors are relatively safe for gastric mucosa, because they have lower ability to inhibit COX-1 expressed in gastric mucosa, resulting in maintenance of gastric level of PGE_2. However, potential risk for cardiovascular thrombotic events is concern. Thus, we propose that NSAIDs with lower cytotoxic effect likely to be therapeutically beneficial NSAIDs in terms of gastrointestinal and cardiovascular safety. We are now synthesizing derivatives of loxoprofen to obtain more safe NSAIDs on gastric mucosa.

Table 1. NSAID Concentrations Required for Apoptosis

NSAIDs	Primary cell (mM)	AGS cell (mM)
Celecoxib	0.06	0.05
Indomethacin	0.42	0.40
Loxoprofen	<20	11.8
Loxoprofen-OH	19.1	4.3

ED_{70} values of NSAIDs for apoptosis (concentrations of NSAIDs required for 70% cell viability by apoptosis) in primary culture of gastric mucosal cells and in AGS cells were calculated based on results provided in Fig. 1 and Fig. 4, respectively.

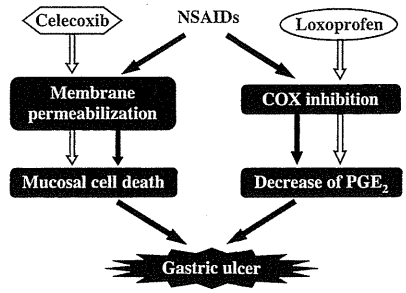

Fig. 5. A Model for Production of Gastric Lesions by NSAIDs

We have proposed that both COX inhibition (decrease in gastric level of PGE_2) and gastric mucosal cell death are required for the formation of NSAID-induced gastric lesions *in vivo*.[20,24] This idea can explain the safety of selective COX-2 inhibitors, such as celecoxib, and loxoprofen on gastric mucosa, because they have lower ability to decrease gastric level of PGE_2 and to induce gastric mucosal cell death, respectively.

Acknowledgements This work was supported by Grants-in-Aid for Scientific Research from the Ministry of Health, Labour, and Welfare of Japan, Grants-in-Aid for Scientific Research from the Ministry of Education, Culture, Sports, Science and Technology of Japan, and Grants-in-Aid of the Japan Science and Technology Agency.

REFERENCES

1) Smalley W. E., Ray W. A., Daugherty J. R., Griffin M. R., *Am. J. Epidemiol.*, **141**, 539—545 (1995).
2) Hawkey C. J., *Gastroenterology*, **119**, 521—535 (2000).
3) Barrier C. H., Hirschowitz B. I., *Arthritis Rheum.*, **32**, 926—932 (1989).
4) Fries J. F., Miller S. R., Spitz P. W., Williams C. A., Hubert H. B., Bloch D. A., *Gastroenterology*, **96**, 647—655 (1989).
5) Kujubu D. A., Fletcher B. S., Varnum B. C., Lim R. W., Herschman H. R., *J. Biol. Chem.*, **266**, 12866—12872 (1991).
6) Xie W. L., Chipman J. G., Robertson D. L., Erikson R. L., Simmons D. L., *Proc. Natl. Acad. Sci. U.S.A.*, **88**, 2692—2696 (1991).
7) Silverstein F. E., Faich G., Goldstein J. L., Simon L. S., Pincus T., Whelton A., Makuch R., Eisen G., Agrawal N. M., Stenson W. F., Burr A. M., Zhao W. W., Kent J. D., Lefkowith J. B., Verburg K. M., Geis G. S., *JAMA*, **284**, 1247—1255 (2000).
8) Bombardier C., Laine L., Reicin A., Shapiro D., Burgos V. R., Davis

B., Day R., Ferraz M. B., Hawkey C. J., Hochberg M. C., Kvien T. K., Schnitzer T. J., *N. Engl. J. Med.*, **343**, 1520—1528, (2000).
9) FitzGerald G. A., Patrono C., *N. Engl. J. Med.*, **345**, 433—442 (2001).
10) Mukherjee D., Nissen S. E., Topol E. J., *JAMA*, **286**, 954—959 (2001).
11) Mukherjee D., *Biochem. Pharmacol.*, **63**, 817—821 (2002).
12) McAdam B. F., Catella L. F., Mardini I. A., Kapoor S., Lawson J. A., FitzGerald G. A., *Proc. Natl. Acad. Sci. U.S.A.*, **96**, 272—277 (1999).
13) Catella L. F., McAdam B., Morrison B. W., Kapoor S., Kujubu D., Antes L., Lasseter K. C., Quan H., Gertz B. J., FitzGerald G. A., *J. Pharmacol. Exp. Ther.*, **289**, 735—741 (1999).
14) Belton O., Byrne D., Kearney D., Leahy A., Fitzgerald D. J., *Circulation*, **102**, 840—845 (2000).
15) Lichtenberger L. M., *Biochem. Pharmacol.*, **61**, 631—637 (2001).
16) Tanaka K., Tomisato W., Hoshino T., Ishihara T., Namba T., Aburaya M., Katsu T., Suzuki K., Tsutsumi S., Mizushima T., *J. Biol. Chem.*, **280**, 31059—31067 (2005).
17) Tsutsumi S., Gotoh T., Tomisato W., Mima S., Hoshino T., Hwang H. J., Takenaka H., Tsuchiya T., Mori M., Mizushima T., *Cell Death Differ.*, **11**, 1009—1016 (2004).
18) Tomisato W., Tanaka K., Katsu T., Kakuta H., Sasaki K., Tsutsumi S., Hoshino T., Aburaya M., Li D., Tsuchiya T., Suzuki K., Yokomizo K., Mizushima T., *Biochem. Biophys. Res. Commun.*, **323**, 1032—1039 (2004).
19) Tomisato W., Tsutsumi S., Rokutan K., Tsuchiya T., Mizushima T., *Am. J. Physiol. Gastrointest. Liver Physiol.*, **281**, G1092—1100 (2001).
20) Aburaya M., Tanaka K., Hoshino T., Tsutsumi S., Suzuki K., Makise M., Akagi R., Mizushima T., *J. Biol. Chem.*, **281**, 33422—33432 (2006).
21) Tsutsumi S., Namba T., Tanaka K. I., Arai Y., Ishihara T., Aburaya M., Mima S., Hoshino T., Mizushima T., *Oncogene*, **25**, 1018—1029 (2006).
22) Namba T., Hoshino T., Tanaka K., Tsutsumi S., Ishihara T., Mima S., Suzuki K., Ogawa S., Mizushima T., *Mol. Pharmacol.*, **71**, 860—870 (2007).
23) Ishihara T., Hoshino T., Namba T., Tanaka K., Mizushima T., *Biochem. Biophys. Res. Commun.*, **356**, 711—717 (2007).
24) Tomisato W., Tsutsumi S., Hoshino T., Hwang H. J., Mio M., Tsuchiya T., Mizushima T., *Biochem. Pharmacol.*, **67**, 575—585 (2004).
25) Misaka E., Yamaguchi T., Iizuka Y., Kamoshida K., Kojima T., Kobayashi K., Endo Y., Misawa Y., Lobayashi S., Tanaka K., *Pharmacometrics*, **21**, 753—771 (1981).
26) Kawano S., Tsuji S., Hayashi N., Takei Y., Nagano K., Fusamoto H., Kamada T., *J. Gastroenterol. Hepatol.*, **10**, 81—85 (1995).
27) Sugimoto M., Kojima T., Asami M., Iizuka Y., Matsuda K., *Biochem. Pharmacol.*, **42**, 2363—2368 (1991).
28) Hirakawa T., Rokutan K., Nikawa T., Kishi K., *Gastroenterology*, **111**, 345—357 (1996).
29) Tomisato W., Takahashi N., Komoto C., Rokutan K., Tsuchiya T., Mizushima T., *Dig. Dis. Sci.*, **45**, 1674—1679 (2000).
30) Tomisato W., Hoshino T., Tsutsumi S., Tsuchiya T., Mizushima T., *Dig. Dis. Sci.*, **47**, 2125—2133 (2002).
31) Tsutsumi S., Tomisato W., Takano T., Rokutan K., Tsuchiya T., Mizushima T., *Biochim. Biophys. Acta*, **1589**, 168—180 (2002).
32) Ushijima H., Tanaka K., Takeda M., Katsu T., Mima S., Mizushima T., *Mol. Pharmacol.*, **68**, 1156—1161 (2005).
33) Katsu T., Kuroko M., Morikawa T., Sanchika K., Yamanaka H., Shinoda S., Fujita Y., *Biochim. Biophys. Acta*, **1027**, 185—190 (1990).
34) Katsu T., Kobayashi H., Hirota T., Fujita Y., Sato K., Nagai U., *Biochim. Biophys. Acta*, **899**, 159—170 (1987).
35) Wang W. H., Huang J. Q., Zheng G. F., Lam S. K., Karlberg J., Wong B. C., *J. Natl. Cancer. Inst.*, **95**, 1784—1791 (2003).
36) Gupta R. A., Dubois R. N., *Nat. Rev. Cancer*, **1**, 11—21 (2001).
37) Kismet K., Akay M. T., Abbasoglu O., Ercan A., *Cancer Detect. Prev.*, **28**, 127—142 (2004).

THE JOURNAL OF BIOLOGICAL CHEMISTRY VOL. 285, NO. 8, pp. 5848–5858, February 19, 2010

Prevention of UVB Radiation-induced Epidermal Damage by Expression of Heat Shock Protein 70*[S]

Received for publication, September 6, 2009, and in revised form, December 7, 2009 Published, JBC Papers in Press, December 14, 2009, DOI 10.1074/jbc.M109.063453

Minoru Matsuda[‡], Tatsuya Hoshino[‡], Yasuhiro Yamashita[‡], Ken-ichiro Tanaka[‡], Daisuke Maji[§], Keizo Sato[‡], Hiroaki Adachi[¶], Gen Sobue[¶], Hironobu Ihn[‡], Yoko Funasaka[‖], and Tohru Mizushima[‡1]

From the [‡]Graduate School of Medical and Pharmaceutical Sciences, Kumamoto University, Kumamoto 862-0973, [§]Saishunkan Pharmaceutical Co., Ltd., Kumamoto 861-2201, the [¶]Nagoya University Graduate School of Medicine, Nagoya 466-8550, and the [‖]Kobe University Graduate School of Medicine, Kobe 650-0017, Japan

Irradiation with UV light, especially UVB, causes epidermal damage via the induction of apoptosis, inflammatory responses, and DNA damage. Various stressors, including UV light, induce heat shock proteins (HSPs) and the induction, particularly that of HSP70, provides cellular resistance to such stressors. The anti-inflammatory activity of HSP70, such as its inhibition of nuclear factor kappa B (NF-κB), was recently revealed. These *in vitro* results suggest that HSP70 protects against UVB-induced epidermal damage. Here we tested this idea by using transgenic mice expressing HSP70 and cultured keratinocytes. Irradiation of wild-type mice with UVB caused epidermal damage such as induction of apoptosis, which was suppressed in transgenic mice expressing HSP70. UVB-induced apoptosis in cultured keratinocytes was suppressed by overexpression of HSP70. Irradiation of wild-type mice with UVB decreased the cutaneous level of IκB-α (an inhibitor of NF-κB) and increased the infiltration of leukocytes and levels of pro-inflammatory cytokines and chemokines in the epidermis. These inflammatory responses were suppressed in transgenic mice expressing HSP70. *In vitro*, the overexpression of HSP70 suppressed the expression of pro-inflammatory cytokines and chemokines and increased the level of IκB-α in keratinocytes irradiated with UVB. UVB induced an increase in cutaneous levels of cyclobutane pyrimidine dimers and 8-hydroxy-2′-deoxyguanosine, both of which were suppressed in transgenic mice expressing HSP70. This study provides genetic evidence that HSP70 protects the epidermis from UVB-induced radiation damage. The findings here also suggest that the protective action of HSP70 is mediated by anti-apoptotic, anti-inflammatory, and anti-DNA damage effects.

The skin can be structurally classified into several layers, including the most apical layer, the epidermis, containing large numbers of keratinocytes, and a second layer, immediately under this, the dermis, which has a high fibroblast content (1). Skin provides a major interface between the environment and the body and is constantly exposed to an array of physical and chemical stressors. Therefore, in addition to intrinsic causes, harmful exogenous causes are involved in the process of skin damage. Among exogenous harmful agents, UV irradiation is the most relevant to skin damage (photo-damage). UV light can be separated, based on wavelength, into three categories: UVA (320–400 nm), UVB (290–320 nm), and UVC (100–290 nm). Of these, the cell-damaging effect of UVA is relatively weak, whereas most UVC is absorbed by the ozone layer (2). Thus, UVB seems to play the central role in photo-damage, such as clinical sunburn, hyperpigmentation, erythema, plaque-like thickening, loss of skin tone, deep furrowing, and fine wrinkle formation, all of which constitute both clinical and cosmetic problems. Furthermore, UVB irradiation induces the development of skin cancer (photo-carcinogenesis) (3). UVB-induced photo-damage and photo-carcinogenesis both involve epidermal damage (such as induction of apoptosis), immunosuppression, inflammation (activation of pro-inflammatory cytokines and chemokines), and DNA damage (4). Because most UVB radiation is absorbed at the epidermis, keratinocytes become a major target of its deleterious effects. For example, the UVB-induced disruption of collagen and elastin (deep furrowing and fine wrinkle formation in the skin) involves inhibition of their synthesis in fibroblasts and stimulation of their degradation by matrix metalloproteinases and other proteases, both of which are triggered by pro-inflammatory cytokines and chemokines released from UVB-irradiated keratinocytes (4, 5). Therefore, suppression of UVB-induced damage (apoptosis) of keratinocytes is beneficial for the prevention of photo-damage. However, because such protection may actually aid in the survival of DNA-damaged cells, resulting in promotion of photo-carcinogenesis, a mechanism that not only suppresses UVB-induced apoptosis but also UVB-induced DNA damage is important to establish protocols to prevent photo-damage without promoting photo-carcinogenesis.

UVB irradiation damages the epidermis both directly and indirectly. For example, in addition to UVB-induced direct damage of nucleic acids, proteins, and lipids, UVB irradiation stimulates the production of reactive oxygen species

* This work was supported by grants-in-aid for scientific research from the Ministry of Health, Labour, and Welfare of Japan, as well as the Japan Science and Technology Agency, grants-in-aid for scientific research from the Ministry of Education, Culture, Sports, Science and Technology, Japan.

[S] The on-line version of this article (available at http://www.jbc.org) contains supplemental Figs. S1–S4.

[1] To whom correspondence should be addressed: Graduate School of Medical and Pharmaceutical Sciences, Kumamoto University, 5-1 Oe-honmachi, Kumamoto 862-0973, Japan. Tel./Fax: 81-96-371-4323; E-mail: mizu@gpo.kumamoto-u.ac.jp.

(ROS),[2] which also damages these molecules by oxidization. In this way, direct absorption of UVB by DNA causes DNA damage through the formation of covalent linkages, resulting in products such as cyclobutane pyrimidine dimers (CPDs). On the other hand, UVB-produced ROS also damage DNA by producing damaged nucleotides such as 8-hydroxy-2′-deoxyguanosine (8-OHdG) (6). Supporting this notion, it was reported that anti-oxidant molecules prevent UVB-induced epidermal DNA damage (7). Thus, mechanisms that protect the epidermis from both UVB and ROS are important to establish ways in which to suppress photodamage efficiently.

When cells are exposed to stressors, a number of so-called stress proteins are induced to confer protection against such stressors. Heat shock proteins (HSPs) are representative of these stress proteins, and their cellular up-regulation of expression, especially that of HSP70, provides resistance given that HSPs re-fold or degrade denatured proteins produced by stressors such as ROS (8, 9). Because stressor-induced tissue damage is involved in various diseases, HSPs and HSP inducers have received much attention for their therapeutic potential. It is known that various HSPs are constitutively expressed in keratinocytes and their expression, especially that of HSP70, is up-regulated by different stressors (10–13). UVB irradiation of keratinocytes induces the expression of HSP70 not only *in vitro* but also *in vivo* (11, 13–17). Furthermore, artificial expression of HSP70 in keratinocytes confers protection against UVB and ROS *in vitro* (8, 16, 18, 19). The protective role of HSP70 against UVB-induced epidermal damage was also suggested by *in vivo* studies: the whole body hyperthermia of mice prevented UVB-induced sunburn cell formation, and HSP70-null mice showed a sensitive phenotype to UVB-induced epidermal damage (20–22). Protection of the skin against UVB by expression of HSP70 has been suggested to occur in human skin (21). These previous results suggest that HSP70 expression suppresses UVB-induced epidermal damage, although no genetic evidence has been reported showing that overproduction of HSP70 prevents UVB-induced epidermal damage.

The potential benefit of HSP70 inducers as medicines for UVB-related skin diseases and cosmetics was also supported by a number of previously reported observations. For example, HSP70 has an anti-inflammatory activity by means of its inhibition of nuclear factor kappa B (NF-κB) and a resulting suppression of pro-inflammatory cytokine and chemokine expression (23–26). HSP70 has been reported to stimulate base excision repair, possibly by activation of human AP endonuclease and DNA polymerase β (27–29). We also recently found that artificial overexpression of HSP70 in mouse melanoma cells suppresses melanin production.[3] Although we showed in that study that the UVB-induced production of melanin in the skin is suppressed in transgenic mice expressing HSP70, the anti-inflammatory and protective effects against DNA damage of HSP70 in UVB-irradiated skin have not been proved genetically. In this study, we examined the protective role of HSP70 against photo-damage by using transgenic mice expressing HSP70. The results obtained here suggest that expression of HSP70 protects the epidermis against UVB-induced damage via anti-inflammatory and anti-apoptotic effects and suppression of DNA damage. Based on these findings, we propose that non-toxic HSP70 inducers could be beneficial for use in cosmetics and medicines for the treatment of UVB-related skin diseases.

EXPERIMENTAL PROCEDURES

Materials and Animals—Paraformaldehyde, 3-(4,5-dimethylthiazol-2-yl)-2,5-diphenyltetrazolium bromide (MTT), peroxidase standard and fetal bovine serum were obtained from Sigma-Aldrich. Enzyme-linked immunosorbent assay kits for interleukin (IL)-1β and IL-6 were from Pierce. Mayer's hematoxylin, 1% eosin alcohol solution, and malinol were from Muto Pure Chemicals (Tokyo, Japan). Terminal nucleotidyltransferase was obtained from Toyobo (Osaka, Japan). The Envision kit was from Dako (Carpinteria, CA). Biotin-14-ATP and Alexa Fluor 488-conjugated streptavidin were purchased from Invitrogen (Carlsbad, CA). VECTASHIELD was from Vector Laboratories. 4′,6-Diamidino-2-phenylindole (DAPI) was from Dojindo Laboratories (Kumamoto, Japan). The RNeasy Fibrous Tissue Mini kit was obtained from Qiagen Inc. (Valencia, CA). The first-strand cDNA synthesis kit was from Takara Bio (Ohtsu, Japan), and IQ SYBR Green Supermix was from Bio-Rad (Hercules, CA). Lipofectamine (TM2000) and pcDNA3.1 plasmid were obtained from Invitrogen. Antibodies against IκB-α and actin were from Santa Cruz Biotechnology (Santa Cruz, CA). An antibody against HSP70 was from Stressgen (Ann Arbor, MI). Antibody against CPDs was from Kamiya Biomedical Co. (Seattle, WA), whereas another against 8-OHdG was from Nikken SEIL (Shizuoka, Japan). α-(4-Pyridyl-1-oxide)-*N*-*tert*-butylnitrone (POBN) was from Alexis (San Diego, CA). Transgenic mice expressing HSP70 and their wild-type counterparts (6–8 weeks old, male) were gifts from Drs. C. E. Angelidis and G. N. Pagoulatos (University of Ioannina, Ioannina, Greece) and were prepared as described previously (30). Homozygotic transgenic mice expressing HSP70 were used in these experiments. The experiments and procedures described here were performed in accordance with the Guide for the Care and Use of Laboratory Animals as adopted and promulgated by the National Institutes of Health and were approved by the Animal Care Committee of Kumamoto University.

UV Irradiation—Animals and cultured cells were exposed to UVB irradiation with a double bank of UVB lamps (peak emission at 312 nm, VL-215LM lamp, Vilber Lourmat). The UV energy was monitored by a radiometer sensor (UVX-31, UV

[2] The abbreviations used are: ROS, reactive oxygen species; CPD, cyclobutane pyrimidine dimer; DAPI, 4,6-diamidino-2-phenylindole dihydrochloride; GGA, geranylgeranylacetone; HSP, heat shock protein; IL, interleukin; IκB-α, an inhibitor of NF-κB; MCP-1, monocyte chemoattractant protein-1; MIP-2, macrophage inflammatory protein-2; MPO, myeloperoxidase; MTT, 3-(4,5-dimethylthiazol-2-yl)-2,5-diphenyltetrazolium bromide; NF-κB, nuclear factor kappa B; 8-OHdG, 8-hydroxy-2′-deoxyguanosine; POBN, α-(4-pyridyl-1-oxide)-*N*-*tert*-butylnitrone; RT, reverse transcription; TUNEL, terminal deoxynucleotidyl transferase-mediated biotinylated UTP nick end labeling.

[3] T. Hoshino, M. Matsuda, Y. Yamashita, M. Takehara, M. Fukuya, K. Mineda, D. Maji, H. Ihn, Y. Funasaka, and T. Mizushima, unpublished data.

Products). Animals were placed under deep anesthesia with chloral hydrate (250 mg/kg), and fur was removed with electric clippers prior to the irradiation.

MPO Activity—Myeloperoxidase (MPO) activity in the skin was measured as described previously (30). Animals were placed under deep ether anesthesia and killed. The skin was dissected, rinsed with cold saline, and cut into small pieces. Samples were homogenized in 50 mM phosphate buffer, freeze-thawed, and centrifuged. The protein concentrations of the supernatants were determined using the Bradford method (31). MPO activity was determined in 10 mM phosphate buffer with 0.5 mM *o*-dianisidine, 0.00005% (w/v) hydrogen peroxide, and 20 μg of protein. MPO activity was obtained from the slope of the reaction curve, and its specific activity was expressed as the number of hydrogen peroxide molecules converted per minute/mg of protein.

Immunoblotting Analysis—Whole cell extracts were prepared as described previously (32). The protein concentration of each sample was determined by the Bradford method (31). Samples were applied to 9% (HSP70 and actin) or 12% (IκB-α) polyacrylamide SDS gels and subjected to electrophoresis, after which the proteins were immunoblotted with appropriate antibodies.

Real-time Reverse Transcription-PCR Analysis—Total RNA was extracted from skin tissues using the RNeasy Fibrous Tissue Mini kit according to the manufacturer's protocol. Samples (2.5 μg of RNA) were reverse-transcribed using the first-strand cDNA synthesis kit according to the manufacturer's instructions. Synthesized cDNA was used in real-time reverse transcription-PCR (Chromo 4 system, Bio-Rad) experiments using iQ SYBR Green Supermix and analyzed with Opticon Monitor software according to the manufacturer's instructions. Specificity was confirmed by electrophoretic analysis of the reaction products and by inclusion of template- or reverse transcriptase-free controls. To normalize the amount of total RNA present in each reaction, glyceraldehyde-3-phosphate dehydrogenase cDNA was used as an internal standard. The primers used were, *hsp70*, 5′-tggtgctgacgaagatgaag-3′ (forward) and 5′-aggtcgaagatgagcacgtt-3′ (reverse); *il-1β*, 5′-gatcccaagcaatacccaaa-3′ (forward) and 5′-ggggaactctgcagactcaa-3′ (reverse); *il-6*, 5′-ctggagtcacagaaggagtgg-3′ (forward) and 5′-ggtttgccgagtagatctcaa-3′ (reverse); monocyte chemoattractant protein-1 (*mcp-1*), 5′-ctcacctgctgctactcattc-3′ (forward) and 5′-gcttgaggtggttgtggaaaa-3′ (reverse); macrophage inflammatory protein-2 (*mip-2*), 5′-accctgccaagggttgacttc-3′ (forward) and 5′-ggcacatcaggtacgatccag-3′ (reverse); and *gapdh*, 5′-aactttggcattgtggaagg-3′ (forward) and 5′-acacattgggggtaggaaca-3′ (reverse).

Histological and Immunohistochemical Analyses and TUNEL Assay—Skin samples were fixed in 4% buffered paraformaldehyde and embedded in paraffin before being cut into 4-μm-thick sections, which were then deparaffinized and washed in phosphate-buffered saline.

For histological examination (hematoxylin and eosin staining), sections were stained first with Mayer's hematoxylin and then with 1% eosin alcohol solution. Samples were mounted with malinol and inspected using a BX51 microscope (Olympus).

For immunohistochemical analyses, sections were incubated with 0.1% (for 8-OHdG) or 0.3% (for CPDs and HSP70) hydrogen peroxide in methanol for removal of endogenous peroxidase. Sections were incubated with 0.125% trypsin in phosphate-buffered saline for 10 min and then with 1 N HCl for 30 min for DNA denaturation. Sections were blocked with 2.5% goat serum for 10 min, incubated for 12 h with antibody against HSP70 (1:200 dilution), 8-OHdG (1:100 dilution), or CPDs (1:500 dilution) in the presence of 2.5% bovine serum albumin, and then incubated for 1 h with peroxidase-labeled polymer conjugated to goat anti-mouse immunoglobulins. 3,3′-Diaminobenzidine was applied to the sections, which were then incubated with Mayer's hematoxylin (hematoxylin staining was omitted for 8-OHdG). Samples were mounted with malinol and inspected using a BX51 microscope (Olympus). The intensity of 8-OHdG staining in the epidermis was measured by LuminaVision (Mitani).

For TUNEL assay, sections were incubated first with proteinase K (20 μg/ml) for 15 min at 37 °C, then with terminal nucleotidyltransferase and biotin-14-ATP for 1 h at 37 °C, and finally with Alexa Fluor 488-conjugated streptavidin and DAPI (5 μg/ml) for 2 h. Samples were mounted with VECTASHIELD and inspected using a BX51 fluorescence microscope (Olympus).

Cell Culture and Apoptosis Analysis—PAM212 cells were cultured in Dulbecco's modified Eagle's medium supplemented with 10% fetal bovine serum in a humidified atmosphere of 95% air with 5% CO_2 at 37 °C. Transfection of PAM212 cells with pcDNA3.1 containing the *hsp70* gene (33) was carried out using Lipofectamine (TM2000) according to the manufacturer's protocol. The stable transfectants expressing HSP70 were selected by immunoblotting and real-time reverse transcription-PCR analyses. Positive clones were maintained in the presence of 200 μg/ml G418. Cell viability was determined by the MTT method as previously described (34), and the measurements of caspase-3-like activity and fluorescence-activated cell sorting analysis (for measurement of apoptotic cells in sub-G_1) were performed as described previously (34).

Immunostaining of 8-OHdG and CPDs in Cultured Cells—Cells were cultured on 8-well Lab-Tek II Chamber slides (Nunc). They were then fixed in methanol for 20 min after UVB irradiation. Cells were permeabilized with 0.5% Triton X-100 for 5 min, treated in a microwave oven with 0.01 M citric acid buffer for antigen activation, and then treated with 1 N HCl for 20 min for DNA denaturation. Cells were blocked with 5% goat serum for 10 min, incubated for 2 h with antibody against 8-OHdG (1:10 dilution) or CPDs (1:2000 dilution) in the presence of 2.5% bovine serum albumin, and finally incubated with Alexa Fluor 488 goat anti-mouse immunoglobulin G. Cells were simultaneously stained with DAPI (5 μg/ml) for 2 h. Samples were mounted with VECTASHIELD and inspected with the aid of a BX51 fluorescence microscope (Olympus). The fluorescence intensity of 8-OHdG or CPD staining was measured by using LuminaVision.

Determination of ROS Production in Vivo by ESR Analysis—*In vivo* ESR analysis was performed as described (35) with some modifications. Immediately after UVB exposure, animals were placed under deep anesthesia with chloral hydrate (250 mg/kg) and injected with POBN (a spin trap reagent) (36, 37) intraperitoneally (4 mmol/kg). After 1 h, mice were sacrificed, the skins

were dissected, and the lipid phase was extracted. After evaporating the sample, ESR spectra were immediately recorded at room temperature using a quartz flat cell (160 μl) in a JES-TE200 spectrometer (JEOL). The operating conditions of the ESR apparatus were: 9.43 GHz, field 335.2 ± 5 milliteslas, 40-milliwatt microwave power, 100-kHz modulation frequency, 0.25-field modulation width, 0.3-s time count, and sweep time of 2 min.

Statistical Analysis—All values are expressed as the means ± S.E. Two-way analysis of variance followed by the Tukey test was used to evaluate differences between more than three groups. Differences were considered to be significant for values of $p < 0.05$.

RESULTS

Effect of Expression of HSP70 on UVB-induced Epidermal Apoptosis—Overexpression of HSP70 in the transgenic mice that we used in this study has been shown in various organs (9, 30, 38–40). We examined HSP70 expression in the skin of these animals as this has not been determined to date. Transgenic mice expressing HSP70 and wild-type mice were irradiated or not with 180 mJ/cm^2 UVB. The dorsal skin was removed 24 h after completion of the irradiation and subjected to immunoblotting analysis. As shown in Fig. 1 (*A* and *B*), the level of HSP70 was significantly higher in transgenic mice than in wild-type mice in both the presence and absence of UVB irradiation. However, under these conditions, UVB irradiation did not up-regulate the expression of HSP70 in either type of mice (Fig. 1, *A* and *B*), a finding that differs from previous reports (20). Although we examined the effect of UVB on expression of HSP70 under various conditions (various doses of UVB and time course of the induction periods), we could not detect the UVB-dependent up-regulation of expression of HSP70 under any conditions by immunoblotting analysis (supplemental Fig. S1). We consider that this is due to the UVB-dependent increase in total amount of proteins (we applied the same amount of proteins in each lane in immunoblotting analysis). Supporting this notion, immunohistochemical analysis with an antibody against HSP70 demonstrated that the expression of HSP70 was induced by UVB irradiation at the skin (the *top panels* in supplemental Fig. S2). Immunohistochemical analysis also demonstrated that the expression of HSP70 is higher in the epidermis than in the dermis, as described previously (11), and that expression in the epidermis is further heightened in transgenic mice (Fig. 1*C*). The results in Fig. 1 suggest that these transgenic mice could be useful for examining the protective role of HSP70 against UVB-induced epidermal damage.

Histological observations revealed extensive infiltration of leukocytes and epidermal disruption in skin sections prepared from UVB-irradiated wild-type mice, whereas the extent of cutaneous damage was not so apparent in transgenic mice expressing HSP70 (Fig. 2*A*). MPO activity, an indicator of the inflammatory infiltration of leukocytes, was increased in wild-type mice in response to the UVB irradiation. This activity was lower in UVB-irradiated transgenic mice expressing HSP70 compared with wild-type mice (Fig. 2*B*). The overexpression of HSP70 in transgenic mice did not affect the background level of MPO activity (Fig. 2*B*). These results show that UVB-induced

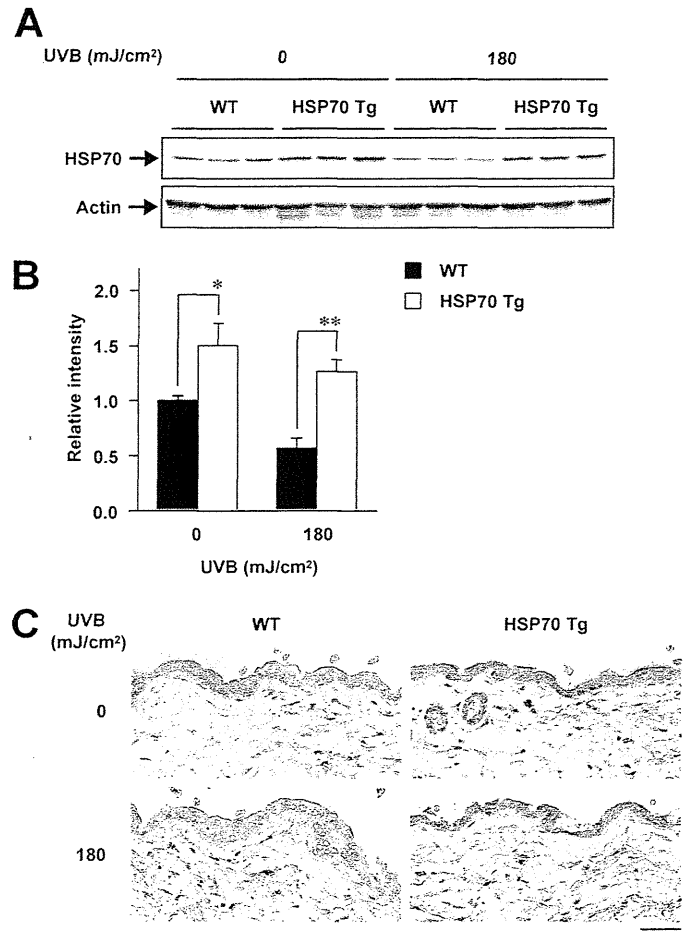

FIGURE 1. **Expression of HSP70 in the dorsal skin after UVB irradiation.** Transgenic mice expressing HSP70 (*HSP70 Tg*) and wild-type mice (*WT*) were irradiated with or without 180 mJ/cm^2 UVB, and the dorsal skin was removed after 24 h. *A*, whole cell extracts were analyzed by immunoblotting with an antibody against HSP70 or actin. *B*, the band intensity of HSP70 was determined and expressed relative to the control sample ($n = 6$) (one of two gels is shown in *panel A*). Values are mean ± S.E. **, $p < 0.01$; *, $p < 0.05$. *C*, sections of dorsal skin were prepared and subjected to immunohistochemical analysis with an antibody against HSP70. *Brown* staining indicates HSP70 expression. *Scale bar*, 50 μm.

epidermal damage and the resulting infiltration of leukocytes are suppressed in transgenic mice expressing HSP70.

The extent of epidermal cell apoptosis was determined by TUNEL assay. An increase of TUNEL-positive (apoptotic) cells in the epidermis of wild-type mice was observed after the UVB irradiation, and this increase was clearly suppressed in transgenic mice expressing HSP70 (Fig. 2, *C* and *D*). The overexpression of HSP70 in transgenic mice did not affect the background level of epidermal apoptosis (Fig. 2, *C* and *D*). These results suggest that the expression of HSP70 protects epidermal cells (keratinocytes) from UVB-induced apoptosis.

To identify cells expressing HSP70 in transgenic mice and wild-type mice irradiated with UVB, we performed co-immunostaining assay. As shown in supplemental Fig. S2, strong co-staining of HSP70 with CD11b (a marker of macrophage) and pan cytokeratin (a marker of keratinocyte) was observed at the skin of transgenic mice expressing HSP70 or wild-type mice irradiated with UVB. A relatively weak co-staining of HSP70 with MPO (a maker of neutrophil) and vimentin (a maker of fibroblast) was also observed (supplemental Fig. S2). These

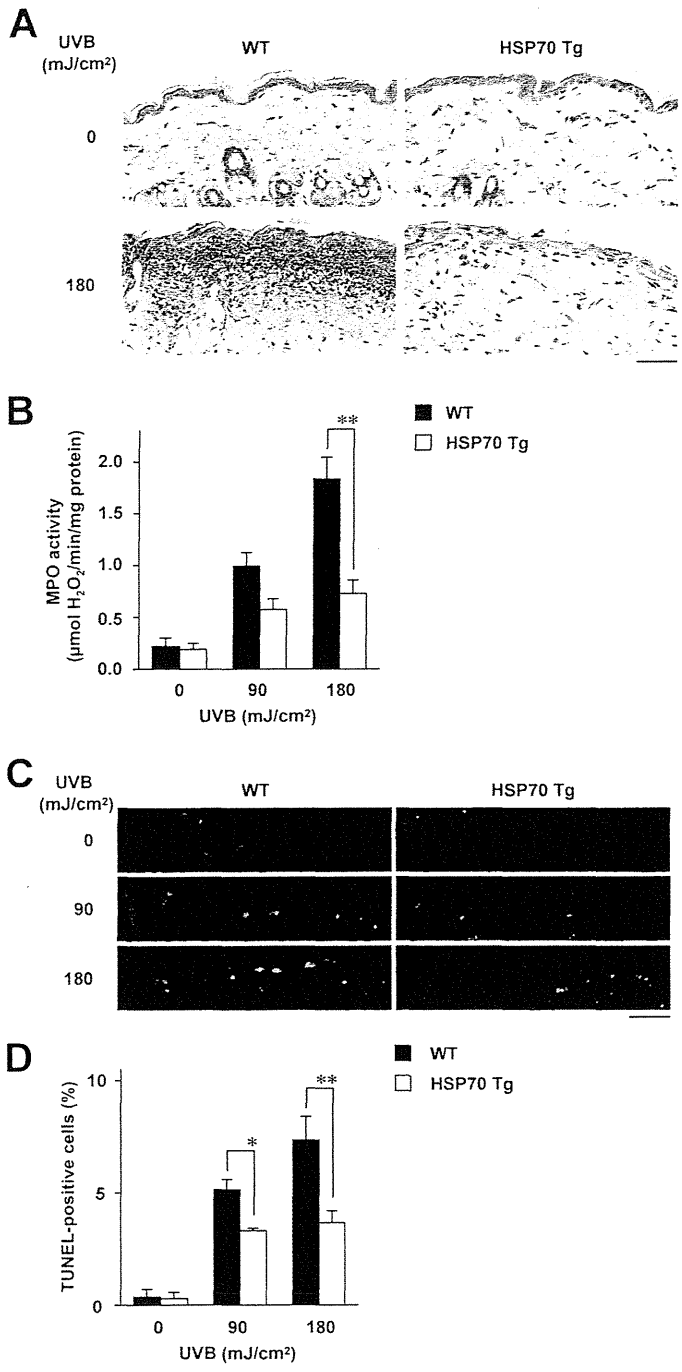

FIGURE 2. **UVB-induced skin damage and apoptosis in wild-type mice and transgenic mice expressing HSP70.** Transgenic mice expressing HSP70 (*HSP70 Tg*) and wild-type mice (*WT*) were irradiated with or without the indicated doses of UVB, and the dorsal skin was removed after 48 h (*A*), 24 h (*B*), or 12 h (*C* and *D*). *A*, sections of dorsal skin were prepared and subjected to hematoxylin and eosin staining. *B*, MPO activity was measured as described under "Experimental Procedures." Values are mean ± S.E. ($n = 8–12$). **, $p < 0.01$. *C*, sections of dorsal skin were subjected to TUNEL assay and DAPI staining. *D*, the ratio of TUNEL-positive cells in the epidermis was counted (400–1000 cells in total). Values are mean ± S.E. ($n = 3$). **, $p < 0.01$; *, $p < 0.05$. *Scale bar*, 50 μm.

results suggest that the transgenic mice and wild-type mice irradiated with UVB express HSP70 in various types of cells at the skin.

We also tried to examine the effect of expression of HSP70 induced by geranylgeranylacetone (GGA), a leading anti-ulcer drug on the Japanese market and an HSP inducer (41). However, as shown in supplemental Fig. S3, GGA did not induce expression of HSP70 by any route of administration (oral, intraperitoneal, and percutaneous administrations). Thus, we used heat treatment to induce expression of HSP70. As shown in supplemental Figs. S3 and S4, heat treatment induced the expression of HSP70 at the skin, and we found that this heat treatment protects the skin from UVB-induced damage (epidermal disruption, increase in MPO activity, and epidermal apoptosis).

To test the idea that the expression of HSP70 protects epidermal cells (keratinocytes) from UVB-induced apoptosis *in vitro*, we constructed a stable transfection of a mouse keratinocyte cell line (PAM212) that continuously overexpresses HSP70 (Clone 2). As shown in Fig. 3*A*, the level of HSP70 in Clone 2 was higher than mock transfectant control cells in both the presence and absence of UVB irradiation. We also found that UVB irradiation up-regulated the expression of HSP70 in both types of cells (Fig. 3*A*). Exposure of cells to UVB irradiation decreased cell viability in a dose-dependent manner; this effect was suppressed in HSP70-overexpressing cells (Fig. 3*B*). To detect UVB-induced apoptosis, we counted cells in sub-G_1 (apoptotic cells) by fluorescence-activated cell sorting analysis. UVB irradiation increased the number of apoptotic cells, and this increase was suppressed in HSP70-overexpressing cells (Table 1). We also monitored apoptosis by measuring caspase-3-like activity using fluorogenic peptide substrates and obtained similar results to those for the fluorescence-activated cell sorting analysis (Table 1). Overexpression of HSP70 did not affect the background level of apoptosis (Table 1). The results in Fig. 3 and Table 1 suggest that the expression of HSP70 helps to protect keratinocytes from UVB-induced apoptosis.

Effect of HSP70 Expression on UVB-induced Epidermal Inflammation—As described above, HSP70 was reported to suppress the activation of NF-κB through various mechanisms such as suppression of the inflammatory stimuli-induced degradation of IκB-α (an inhibitor of NF-κB) (26). We therefore examined the effect of UVB irradiation and/or expression of HSP70 on the level of IκB-α both *in vivo* and *in vitro*. As shown in Fig. 4 (*A* and *B*), UVB irradiation decreased the cutaneous level of IκB-α both in wild-type mice and in transgenic mice expressing HSP70, although the level remained significantly higher in the latter. We also compared the mRNA expression of pro-inflammatory cytokines (IL-1β and IL-6) and chemokines (MIP-2 and MCP-1) between UVB-irradiated transgenic mice expressing HSP70 and wild-type mice. The mRNA expression of *il-1β*, *il-6*, *mip-2*, and *mcp-1* was increased by UVB irradiation, but this increase was much lower in skin samples prepared from transgenic mice expressing HSP70 compared with samples from wild-type mice (Table 2*A*). The expression of HSP70 in transgenic mice did not affect the background levels of mRNA expression (Table 2*A*). Similar results were observed for the protein levels of cytokines (IL-1β and IL-6) determined by enzyme-linked immunosorbent assay (Table 2*B*). The results in Fig. 4 and Table 2 suggest that expression of HSP70 in the skin suppresses the UVB-induced expression of cytokines and chemokines via the inhibition of IκB-α degradation and the resulting suppression of NF-κB activity.

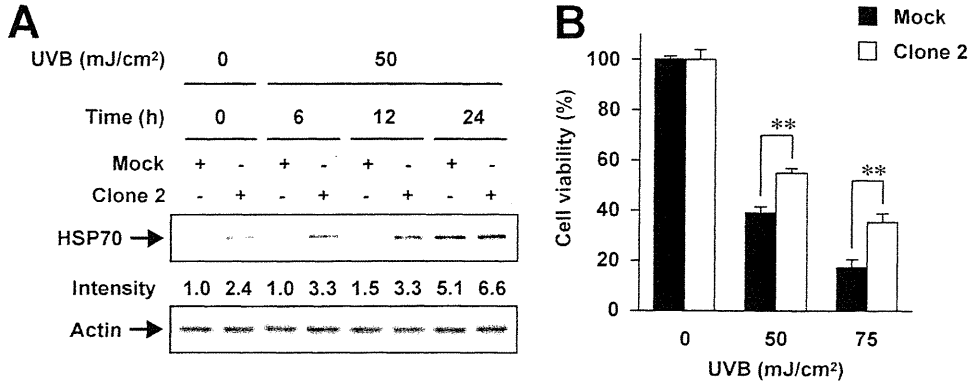

FIGURE 3. **Effect of HSP70 expression on UVB-induced apoptosis *in vitro*.** HSP70-overexpressing PAM212 cells (*Clone 2*) and mock transfectant control cells (*Mock*) were irradiated with or without indicated doses of UVB and cultured for indicated periods (*A*) or 24 h (*B*). *A*, whole cell extracts were subjected to immunoblotting with an antibody against HSP70 or actin. The relative HSP70 band intensity is shown *under the band*. *B*, cell viability was determined by the MTT method. Values are mean ± S.E. ($n = 3$). **, $p < 0.01$.

TABLE 1

Effect of HSP70 expression on UVB-induced apoptosis *in vitro*

HSP70-overexpressing PAM212 cells (Clone 2 in Fig. 3) and mock transfectant control cells (Mock) were irradiated with or without indicated doses of UVB and cultured for 24 h. Apoptotic cells (cells in sub-G_1) were counted by fluorescence-activated cell sorting. Caspase-3-like activity was measured. Values are mean ± S.E. ($n = 3$).

UVB	Cells in sub-G_1		Caspase-3-like activity	
	Mock	Clone 2	Mock	Clone 2
mJ/cm²	%		*Units/mg protein*	
0	2.8 ± 0.37	1.6 ± 0.24	14.2 ± 2.5	27.6 ± 5.7
50	19.2 ± 0.26	10.3 ± 0.18[a]	762.9 ± 19.0	601.7 ± 29.3[a]
75	65.2 ± 1.40	24.4 ± 0.28[a]	1316.9 ± 7.4	700.7 ± 12.6[a]

[a] $p < 0.01$.

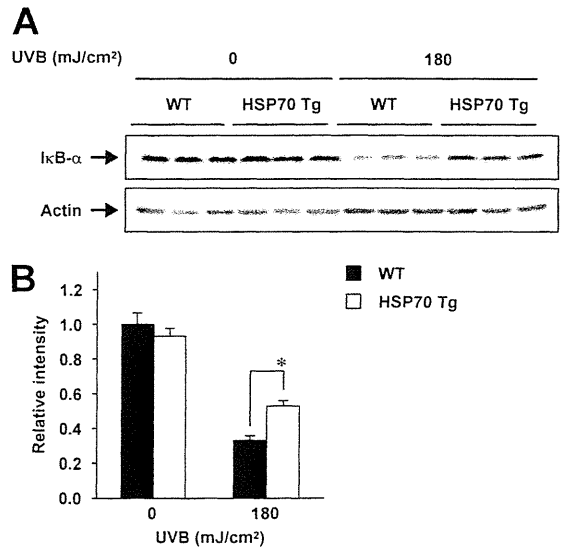

FIGURE 4. **UVB-induced decrease in the level of IκB-α.** Transgenic mice expressing HSP70 (*HSP70 Tg*) and wild-type mice (*WT*) were irradiated with or without 180 mJ/cm² UVB. *A*, the dorsal skin was removed after 48 h, and whole cell extracts were analyzed by immunoblotting with an antibody against IκB-α or actin. *B*, the band intensity of IκB-α was determined and expressed relative to the control sample (one of two gels is shown in *panel A*). Values are mean ± S.E. ($n = 6$). *, $p < 0.05$.

To test this notion *in vitro*, we examined the effect of UVB irradiation and/or expression of HSP70 in cultured keratinocytes on the degradation of IκB-α and expression of just one pro-inflammatory cytokine (IL-6, it has been reported that IL-1β is not expressed in mouse keratinocytes (42, 43)) and chemokines (MIP-2 and MCP-1). As shown in Fig. 5*A*, UVB irradiation transiently (at 6–12 h after the UVB irradiation) decreased the level of IκB-α, and this level was higher in HSP70-overexpressing cells than in mock transfectant control cells at any period after the UVB irradiation. Expression of HSP70 increased the background level of IκB-α (Fig. 5*A*), these results being different from those observed *in vivo* (Fig. 4*A*). Furthermore, expression of the pro-inflammatory cytokine and chemokine genes tested (*il-6*, *mip-2*, and *mcp-1*) was up-regulated by the UVB irradiation, although the expression was suppressed in UVB-irradiated HSP70-overexpressing cells compared with mock transfectant control cells (Fig. 5*B*). Overexpression of HSP70 suppressed the background expression of *mcp-1* but not *il-6* and *mip-2* genes (Fig. 5*B*). The results in Fig. 5 support the notion that the expression of HSP70 in keratinocytes suppresses the UVB-induced expression of cytokines and chemokines via the inhibition of IκB-α degradation and the resulting suppression of NF-κB activity.

Effect of HSP70 Expression on UVB-induced Epidermal DNA Damage—As described in the introduction, UVB irradiation damages DNA (formation of photo-products) directly (formation of products such as CPDs) and indirectly via the production of ROS (formation of products such as 8-OHdG). To examine the effect of HSP70 expression on UVB-induced DNA damage in the epidermis, we compared the time-course profile of the level of CPDs and 8-OHdG after irradiation with UVB between transgenic mice expressing HSP70 and wild-type mice. As shown in Fig. 6 (*A* and *B*), the level of 8-OHdG, judged from the intensity of immunohistochemical staining, was significantly lower in the epidermis of UVB-irradiated transgenic mice expressing HSP70 than in wild-type mice 1 h after the UVB irradiation (45 mJ/cm^2), suggesting that the UVB-induced formation of 8-OHdG is suppressed in the transgenic mice. Although the level of 8-OHdG 1 h after the irradiation was similar between wild-type mice irradiated with 45 mJ/cm^2 UVB and transgenic mice irradiated with 55 mJ/cm^2 UVB, the level was significantly lower in transgenic mice than in wild-type mice 48 h after the irradiation (Fig. 6, *A* and *B*), suggesting that the repair process of 8-OHdG is stimulated in transgenic mice expressing HSP70.

We also measured the level of CPDs in a similar manner. As shown in Fig. 6 (*C* and *D*), the number of CPD-positive cells was similar between wild-type mice and transgenic mice 1 h after the UVB irradiation. On the other hand, the number was significantly lower in transgenic mice than in wild-type mice 24 or 48 h after the UVB irradiation (Fig. 6, *C* and *D*). The results suggest that the repair rather than the formation of CPDs is affected by the expression of HSP70.

We then tested whether or not the effect of HSP70 expression on the formation and repair of 8-OHdG and CPDs can be reproduced *in vitro*. HSP70-overexpressing PAM212 cells and

mock transfectant control cells were irradiated with UVB, and the nuclear levels of 8-OHdG and CPDs were monitored by immunostaining. As shown in Fig. 7, *A* and *B*, HSP70-overexpressing cells showed a lower level of 8-OHdG than mock transfectant control cells 5 min after the UVB irradiation (50 mJ/cm^2), suggesting that the formation of 8-OHdG is suppressed by the expression of HSP70. Furthermore, comparing the level of 8-OHdG between HSP70-overexpressing cells irradiated with 65 mJ/cm^2 UVB and mock transfectant control cells irradiated with 50 mJ/cm^2 UVB, the initial (5 min after the UVB irradiation) levels were indistinguishable; however, the level was lower in HSP70-overexpressing cells than in mock transfectant control cells 24 h after the irradiation (Fig. 7, *A* and *B*), suggesting that the repair process of 8-OHdG is stimulated by the expression of HSP70. In other words, the protective effect of HSP70 against UVB-induced formation of 8-OHdG and its simulative effect on the repair process can be reproduced *in vitro*. On the other hand, the level of CPDs was indistinguishable between HSP70-overexpressing cells and mock transfectant control cells both 5 min and 24 h after the UVB irradiation, suggesting that neither the formation nor repair of CPDs is affected by the expression of HSP70. That is to say, the effect of HSP70 on the repair of CPDs was not reproduced *in vitro*.

The results in Fig. 6, *A* and *B*, suggest that UVB-induced ROS production in the skin is suppressed in transgenic mice expressing HSP70. On this basis, we measured the level of ROS in the skin by monitoring the lipid-derived free radical spin adduct with ESR spectroscopy and spin trap POBN, which reacts with ROS to form a radical spin adduct. As shown in Fig. 8*A*, a radical spin adduct of ESR spectrum similar to that reported in other organs was obtained (35–37, 44). The hyperfine coupling constants for the POBN radical adducts were $\alpha^N = 14.91 \pm 0.08$ G and $\alpha_b^H = 2.45 \pm 0.04$ G, which are similar to data previously reported for other organs (35–37, 44), suggesting that this ESR spectrum is derived from lipid-derived free radicals. As shown in Fig. 8*B*, the level of ROS in the skin was elevated by UVB irradiation in wild-type mice, and this increase was suppressed in transgenic mice expressing HSP70. This finding suggests that the expression of HSP70 suppresses UVB-induced ROS production in the skin.

TABLE 2

UVB-induced expression of pro-inflammatory cytokines and chemokines

Transgenic mice expressing HSP70 (HSP70 Tg) and wild-type mice (WT) were irradiated with or without 180 mJ/cm^2 UVB. In A, the dorsal skin was removed after 12 h (*mip-2*), 24 h (*il-6*, *mcp-1*), or 48 h (*il-1β*), and total RNA was extracted. Samples were subjected to real-time RT-PCR using a specific primer set for each gene. Values were normalized to the *gapdh* gene, expressed relative to the control sample. In B, the dorsal skin was removed after 48 h and skin homogenates were prepared. The amount of IL-1β and IL-6 was determined by using enzyme-linked immunosorbent assay. Values are mean ± S.E. (n = 6–9).

	UVB (mJ/cm^2)	WT	HSP70 Tg
A) Relative expression			
il-1β	0	1.0 ± 0.11	1.6 ± 0.31
	180	24.7 ± 9.19	3.4 ± 0.10[a]
il-6	0	1.0 ± 0.17	0.48 ± 0.072
	180	10.6 ± 1.66	5.6 ± 0.92[a]
mip-2	0	1.0 ± 0.89	1.8 ± 1.62
	180	16.7 ± 1.13	8.3 ± 0.55[b]
mcp-1	0	1.0 ± 0.46	1.5 ± 0.32
	180	36.7 ± 0.40	15.1 ± 6.00[a]
B) ng/g tissue			
IL-1β	0	0.48 ± 0.12	0.84 ± 0.14
	180	27.9 ± 2.71	8.7 ± 1.00[a]
IL-6	0	1.2 ± 0.37	0.87 ± 0.19
	180	67.4 ± 1.66	36.4 ± 5.93[a]

[a] $p < 0.01$.
[b] $p < 0.05$.

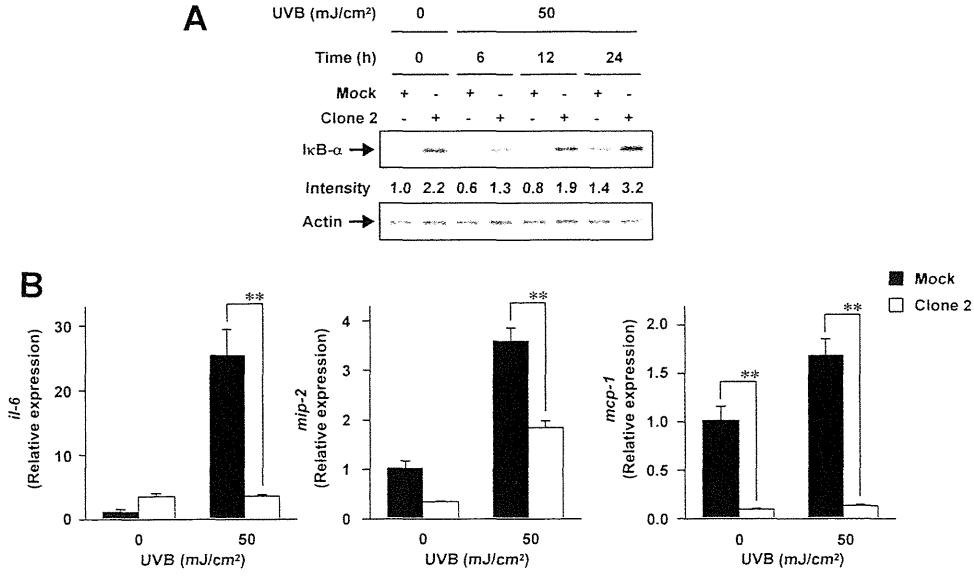

FIGURE 5. **Effect of HSP70 expression on UVB-induced decrease in the level of IκB-α and expression of pro-inflammatory cytokines and chemokines *in vitro*.** HSP70-overexpressing PAM212 cells (*Clone 2*) and mock transfectant control cells (*Mock*) were irradiated with or without 50 mJ/cm^2 UVB and incubated for indicated periods (*A*) or 6 h (*mip-2*), 12 h (*il-6*), or 24 h (*mcp-1*) (*B*). *A*, the expression of IκB-α was estimated by immunoblotting and shown as described in the legend of Fig. 3. *B*, mRNA expression of each gene was monitored as described in the legend of Table 2. Values are mean ± S.E. (n = 3). **, $p < 0.01$.

DISCUSSION

An ameliorative effect of HSP70 due to its cytoprotective, anti-inflammatory, and molecular chaperone (quality control of proteins) properties has been reported for various diseases. For example, we have shown using transgenic mice that HSP70 protects against irritant-produced lesions in the stomach and small intestine and inflammatory bowel disease-related experimental colitis (30, 38–40). The potential therapeutic applicability of HSP70 for use in other diseases, such as neurodegenerative diseases, ischemia-reperfusion damage, and diabetes has also been suggested (9, 45). Interestingly, GGA, a leading anti-ulcer drug on the Japanese market, has been reported to be an HSP inducer, up-regulating various HSPs not only in cultured gastric mucosal cells but also in various tissues *in vivo* (41). It was reported that GGA suppresses not only gastric lesions but also lesions of the small intestine, inflammatory bowel disease-related experimental colitis, and neurodegenerative diseases (39, 40, 46, 47). On the other hand, the use of HSP70 inducers in cosmetics

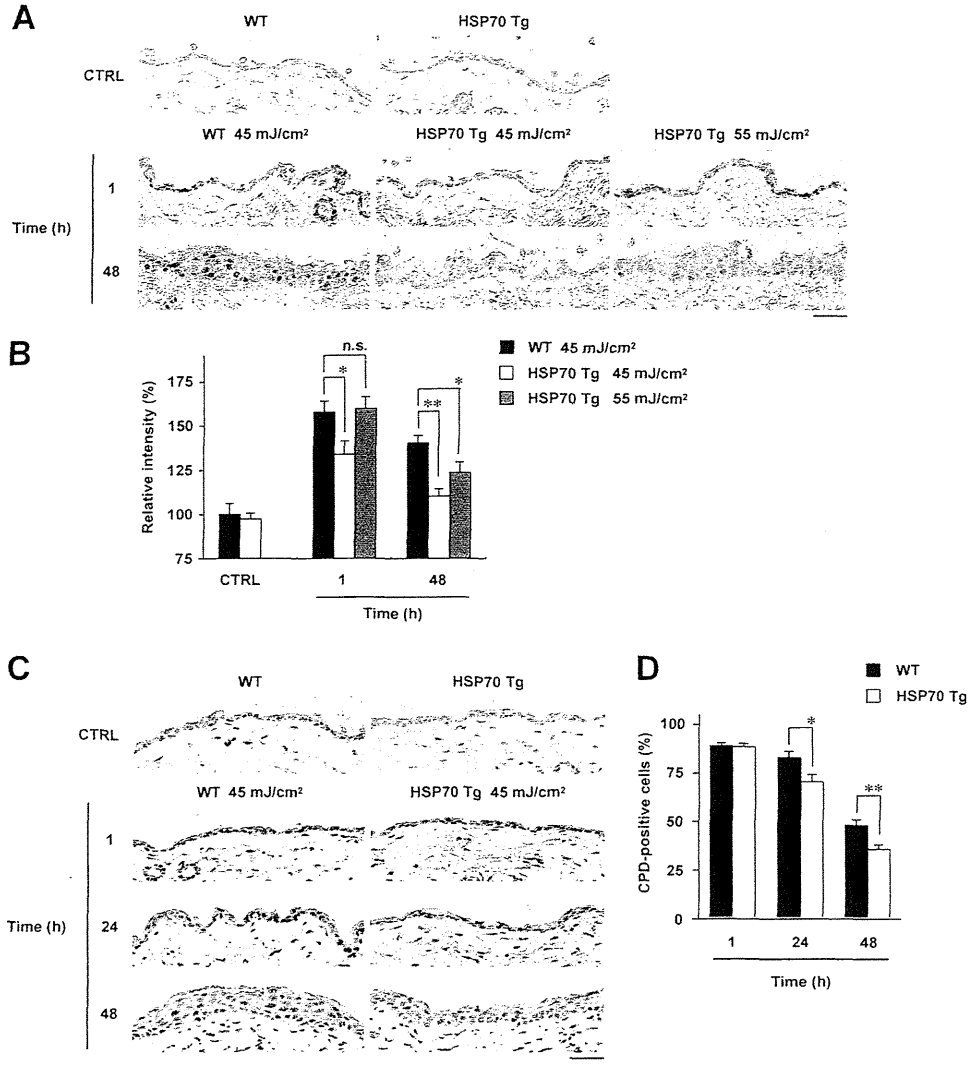

FIGURE 6. **UVB-induced epidermal DNA damage.** Transgenic mice expressing HSP70 (*HSP70 Tg*) and wild-type mice (*WT*) were irradiated with or without (*CTRL*) indicated doses (*A* and *B*) or 45 mJ/cm^2 (*C* and *D*) of UVB. Sections of the dorsal skin were prepared after indicated periods and subjected to immunohistochemical analysis with an antibody against 8-OHdG (*A*) or CPDs (*C*). The intensity of 8-OHdG-staining (*B*) and the percentage of CPD-positive cells (400–600 cells in total) (*D*) were measured. *B* and *D*, values are mean ± S.E. (n = 6). **, $p < 0.01$; *, $p < 0.05$; *n.s.*, not significant. *Scale bar*, 50 μm.

We showed here that UVB-induced apoptosis was suppressed in the epidermis of transgenic mice and in cultured keratinocytes overexpressing HSP70. These results are basically consistent with previous results (8, 16, 18, 20–22). It was suggested that HSP70 suppresses various steps in the molecular pathways governing apoptosis, including p53 activation, which plays an important role in UVB-induced apoptosis (50, 51). In addition to this anti-apoptotic (cytoprotective) effect of HSP70, an anti-inflammatory effect (suppression of NF-κB activity) was recently revealed and thought to be important for HSP70 function (24–26). However, it was not clear whether HSP70 suppresses the activity of NF-κB *in vivo*. In this study, we confirmed that expression of HSP70 increases the level of IκB-α (an inhibitor of NF-κB) *in vitro* and found that a UVB-induced decrease in the level of IκB-α in the skin is suppressed in transgenic mice expressing HSP70. We also showed that the UVB-induced expression of pro-inflammatory cytokines and chemokines is suppressed in transgenic mice expressing HSP70. These results suggest that HSP70 expression in the skin suppresses inflammation via the inhibition of NF-κB activity and the resulting inhibition of pro-inflammatory cytokine and chemokine expression. Considering the adverse effects of inflammation on various skin diseases, these properties of HSP70 could make the development of HSP70 inducers an important advance in the search for medicines to cure UVB-related skin diseases.

and medicines to aid in the treatment of UVB-related skin diseases has not been fully evaluated. A number of *in vitro* studies suggested that HSP70 protects keratinocytes from UVB irradiation; however, the protective role of HSP70 against UVB-induced functional and structural alterations of the epidermis has not been proved genetically. In this study, using transgenic mice overexpressing HSP70, we have shown that the expression of HSP70 suppresses UVB-induced epidermal apoptosis, inflammatory responses, ROS production, and DNA damage, suggesting that HSP70 inducers could be beneficial for use as agents in medicines and cosmetics to alleviate the symptoms and/or cure UVB-related skin diseases. These effects of HSP70 should be mutually dependent. For example, ROS stimulate NF-κB activity and DNA damage, and both ROS and DNA damage induce apoptosis (48, 49). Our results also suggest that the high level of constitutive expression of HSP70 in keratinocytes could play an important role in protecting the skin against UVB irradiation.

We also showed that the UVB-induced increase in levels of both CPDs (UVB-induced direct DNA damage) and 8-OHdG (UVB-dependent indirect DNA damage via the production of ROS) is suppressed in transgenic mice expressing HSP70. This is the first *in vivo* evidence of the protective effect of HSP70 against UVB-induced DNA damage to the skin. This finding is particularly important, because UVB-induced DNA damage plays an important role in UVB-induced skin diseases, especially carcinogenesis. Because HSP70 protects epidermal cells from UVB-induced apoptosis, it could also in fact stimulate skin carcinogenesis by aiding the survival of DNA-damaged cells. However, a further beneficial effect of HSP70 (suppression of UVB-induced DNA damage) may circumvent this problem. The formation and repair of 8-OHdG have been suggested to be

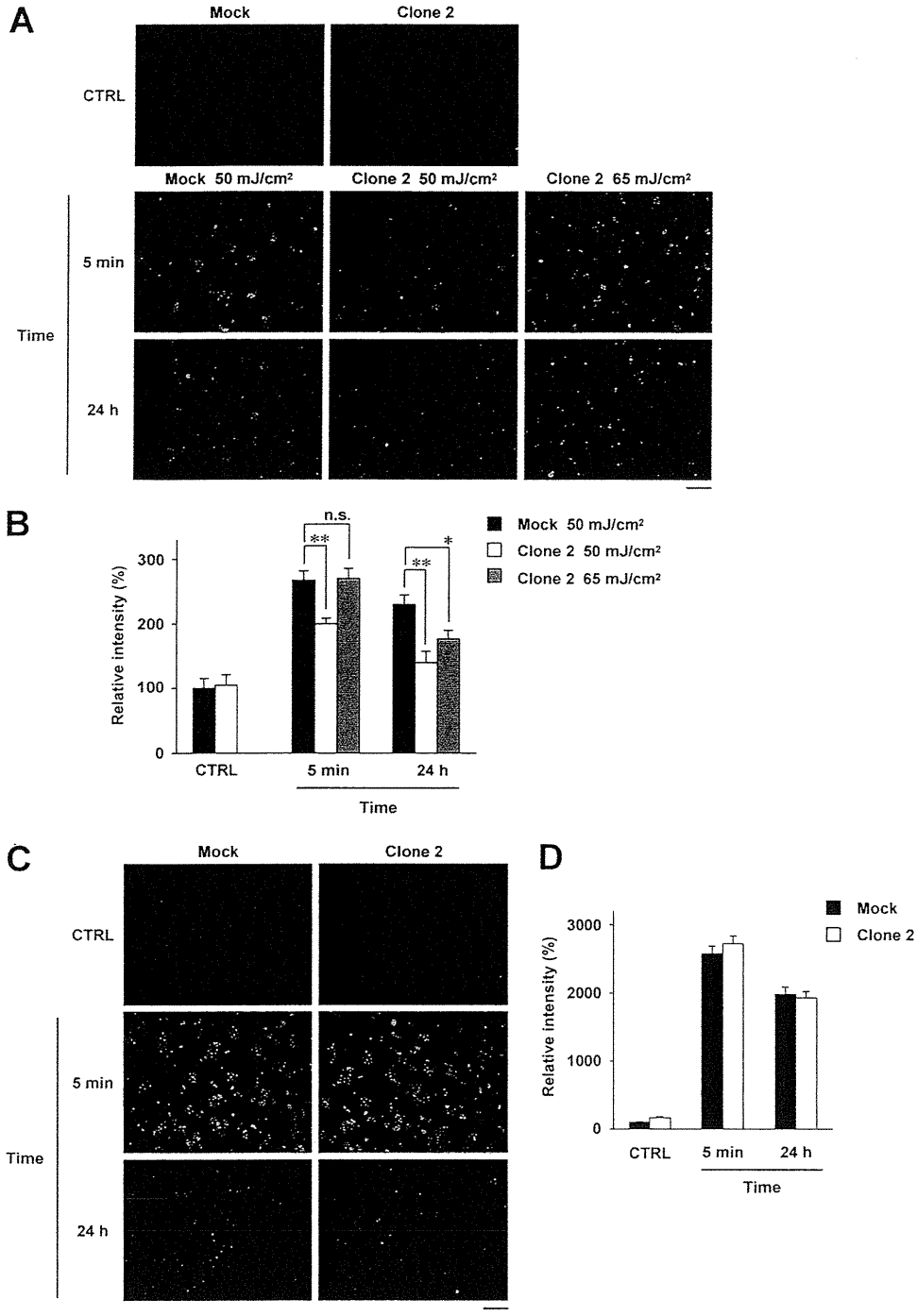

FIGURE 7. **Effect HSP70 expression on UVB-induced DNA damage *in vitro*.** HSP70-overexpressing PAM212 cells (*Clone 2*) and mock transfectant control cells (*Mock*) were irradiated with or without (*CTRL*) indicated doses (*A* and *B*) or 50 mJ/cm^2 (*C* and *D*) of UVB and cultured for indicated periods. Cells were subjected to immunostaining analysis with an antibody against 8-OHdG (*A*) or CPDs (*C*). The fluorescence intensity of 8-OHdG (*B*) and CPDs (*D*) staining was measured. *B* and *D*, values are mean ± S.E. ($n = 6$). **, $p < 0.01$; *, $p < 0.05$; *n.s.*, not significant. *Scale bar*, 100 μm.

suppressed and stimulated, respectively, in transgenic mice expressing HSP70. We also reproduced those findings in cultured keratinocytes, suggesting that HSP70 expressed in these cells is directly responsible for these phenomena. HSP70 seems to suppress the formation of 8-OHdG by decreasing the level of ROS, because the UVB-induced increase in the level of ROS was suppressed in transgenic mice expressing HSP70. A decrease in the level of ROS due to the increased expression of HSP70 was also reported *in vitro* (52). HSP70 stimulates base excision repair, possibly via the activation of human AP endonuclease and DNA polymerase β (27–29). This effect may be involved in an HSP70-dependent stimulation of the 8-OHdG repair process, because the base excision repair system plays a major role in the repair of 8-OHdG (6). On the other hand, although our *in vivo* results suggested that the repair process of CPDs is stimulated by the expression of HSP70, we could not reproduce these results *in vitro*. However, a slight up-regulation of CPD repair by the expression of HSP70 was reported elsewhere (53). Furthermore, in *Escherichia coli*, an HSP70 homologue (DnaK) stimulates the nucleotide excision repair of damaged DNA (54), which plays a major role in the repair of CPDs (6).

We recently found that the artificial expression of HSP70 in cultured melanoma cells suppresses melanin production,[3] suggesting that HSP70 inducers could be beneficial for use as hypopigmenting cosmetics and medicines. A number of compounds that inhibit melanin production have been discovered, however most of their cosmetic and pharmaceutical applications have not been successful due to the occurrence of skin irritation (55), which is caused by the fact that UV-induced mild melanogenesis has a protective role against UVB-induced skin damage, especially DNA damage. Melanin also acts as a scavenger of the UVB-induced production of ROS (56). Therefore, the findings in this study that HSP70 expression suppresses both UVB-induced epidermal DNA damage and the increase in the cutaneous level of ROS are important for the development HSP70 inducers as hypopigmenting cosmetics and medicines. The anti-inflammatory effects of HSP70 may help in this manner, because UVB-induced inflammation actually stimulates pigmentation (57). Based on these results, we propose that HSP70 inducers could have numerous cosmetically and pharmaceutically beneficial applications. We have already screened for HSP70 inducers from Chinese herbal extracts and

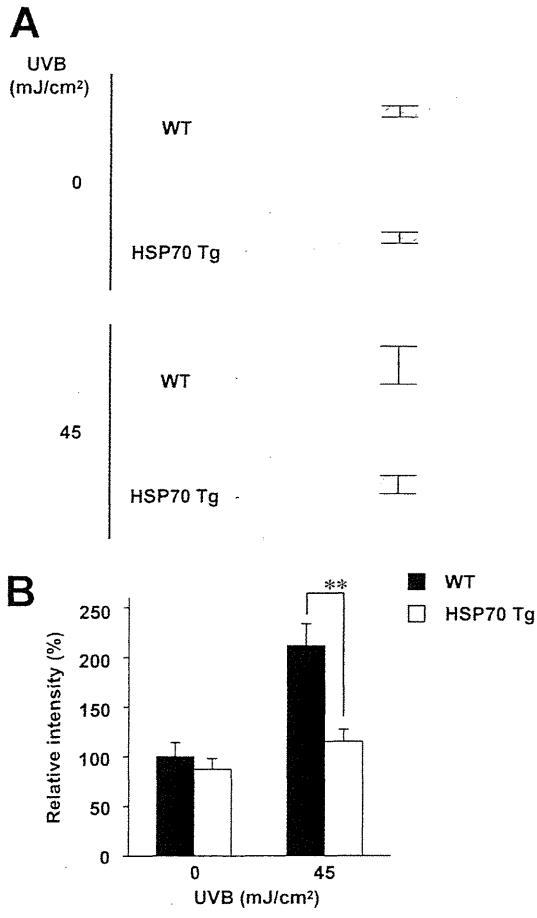

FIGURE 8. **UVB-induced increase in the epidermal ROS level.** Transgenic mice expressing HSP70 (*HSP70 Tg*) and wild-type mice (*WT*) were irradiated with 45 mJ/cm^2 UVB. *A*, POBN was administered, and the dorsal skin was removed after 1 h and subjected to radical adduct ESR spectrum analysis. *B*, the intensity of the ESR signal of the radical adduct (shown by the *bar* in *A*) was determined, expressed relative to the control sample, and given as the mean ± S.E. (n = 6–10). **, $p < 0.01$.

found that their HSP70-inducing activities were more potent than GGA.[4] We hope to develop some of these extracts as hypopigmenting (whitening) cosmetics or as drugs to combat melanin-related diseases.

Acknowledgments—We thank Drs. C. E. Angelidis and G. N. Pagoulatos (University of Ioannina, Greece) for generously providing transgenic mice expressing HSP70.

REFERENCES

1. Rabe, J. H., Mamelak, A. J., McElgunn, P. J., Morison, W. L., and Sauder, D. N. (2006) *J. Am. Acad. Dermatol.* **55,** 1–19
2. Svobodova, A., Walterova, D., and Vostalova, J. (2006) *Biomed. Pap. Med. Fac. Univ. Palacky. Olomouc. Czech. Repub.* **150,** 25–38
3. Matsumura, Y., and Ananthaswamy, H. M. (2004) *Toxicol. Appl. Pharmacol.* **195,** 298–308
4. Gröne, A. (2002) *Vet. Immunol. Immunopathol.* **88,** 1–12
5. Fisher, G. J., Wang, Z. Q., Datta, S. C., Varani, J., Kang, S., and Voorhees, J. J. (1997) *N. Engl. J. Med.* **337,** 1419–1428
6. Hoeijmakers, J. H. (2001) *Nature* **411,** 366–374
7. Budiyanto, A., Ahmed, N. U., Wu, A., Bito, T., Nikaido, O., Osawa, T., Ueda, M., and Ichihashi, M. (2000) *Carcinogenesis* **21,** 2085–2090
8. Simon, M. M., Reikerstorfer, A., Schwarz, A., Krone, C., Luger, T. A., Jäättelä, M., and Schwarz, T. (1995) *J. Clin. Invest.* **95,** 926–933
9. Morimoto, R. I., and Santoro, M. G. (1998) *Nat. Biotechnol.* **16,** 833–838
10. Wilson, N., McArdle, A., Guerin, D., Tasker, H., Wareing, P., Foster, C. S., Jackson, M. J., and Rhodes, L. E. (2000) *J. Cutan. Pathol.* **27,** 176–182
11. Morris, S. D. (2002) *Clin. Exp. Dermatol.* **27,** 220–224
12. Trautinger, F., Trautinger, I., Kindås-Mügge, I., Metze, D., and Luger, T. A. (1993) *J. Invest. Dermatol.* **101,** 334–338
13. Jonak, C., Klosner, G., and Trautinger, F. (2006) *Int. J. Cosmet. Sci.* **28,** 233–241
14. Zhou, X., Tron, V. A., Li, G., and Trotter, M. J. (1998) *J. Invest. Dermatol.* **111,** 194–198
15. Trautinger, F., Kokesch, C., Klosner, G., Knobler, R. M., and Kindås-Mügge, I. (1999) *Exp. Dermatol.* **8,** 187–192
16. Trautinger, F. (2001) *J. Photochem. Photobiol. B* **63,** 70–77
17. Brunet, S., and Giacomoni, P. U. (1989) *Mutat. Res.* **219,** 217–224
18. Trautinger, F., Kindås-Mügge, I., Barlan, B., Neuner, P., and Knobler, R. M. (1995) *J. Invest. Dermatol.* **105,** 160–162
19. Maytin, E. V., Wimberly, J. M., and Kane, K. S. (1994) *J. Invest. Dermatol.* **103,** 547–553
20. Kwon, S. B., Young, C., Kim, D. S., Choi, H. O., Kim, K. H., Chung, J. H., Eun, H. C., Park, K. C., Oh, C. K., and Seo, J. S. (2002) *J. Dermatol. Sci.* **28,** 144–151
21. Trautinger, F., Knobler, R. M., Hönigsmann, H., Mayr, W., and Kindås-Mügge, I. (1996) *J. Invest. Dermatol.* **107,** 442–443
22. Kane, K. S., and Maytin, E. V. (1995) *J. Invest. Dermatol.* **104,** 62–67
23. Krappmann, D., Wegener, E., Sunami, Y., Esen, M., Thiel, A., Mordmuller, B., and Scheidereit, C. (2004) *Mol. Cell. Biol.* **24,** 6488–6500
24. Tang, D., Kang, R., Xiao, W., Wang, H., Calderwood, S. K., and Xiao, X. (2007) *J. Immunol.* **179,** 1236–1244
25. Chen, H., Wu, Y., Zhang, Y., Jin, L., Luo, L., Xue, B., Lu, C., Zhang, X., and Yin, Z. (2006) *FEBS Lett.* **580,** 3145–3152
26. Weiss, Y. G., Bromberg, Z., Raj, N., Raphael, J., Goloubinoff, P., Ben-Neriah, Y., and Deutschman, C. S. (2007) *Crit. Care. Med.* **35,** 2128–2138
27. Bases, R. (2006) *Cell Stress Chaperones* **11,** 240–249
28. Kenny, M. K., Mendez, F., Sandigursky, M., Kureekattil, R. P., Goldman, J. D., Franklin, W. A., and Bases, R. (2001) *J. Biol. Chem.* **276,** 9532–9536
29. Mendez, F., Kozin, E., and Bases, R. (2003) *Cell Stress Chaperones* **8,** 153–161
30. Tanaka, K., Namba, T., Arai, Y., Fujimoto, M., Adachi, H., Sobue, G., Takeuchi, K., Nakai, A., and Mizushima, T. (2007) *J. Biol. Chem.* **282,** 23240–23252
31. Bradford, M. M. (1976) *Anal. Biochem.* **72,** 248–254
32. Hoshino, T., Tsutsumi, S., Tomisato, W., Hwang, H. J., Tsuchiya, T., and Mizushima, T. (2003) *J. Biol. Chem.* **278,** 12752–12758
33. Fujimoto, M., Takaki, E., Hayashi, T., Kitaura, Y., Tanaka, Y., Inouye, S., and Nakai, A. (2005) *J. Biol. Chem.* **280,** 34908–34916
34. Namba, T., Hoshino, T., Tanaka, K., Tsutsumi, S., Ishihara, T., Mima, S., Suzuki, K., Ogawa, S., and Mizushima, T. (2007) *Mol. Pharmacol.* **71,** 860–870
35. Ishihara, T., Tanaka, K., Tasaka, Y., Namba, T., Suzuki, J., Ishihara, T.,O-kamoto, S., Hibi, T., Takenaga, M., Igarashi, R., Sato, K., Mizushima, Y., and Mizushima, T. (2009) *J. Pharmacol. Exp. Ther.* **328,** 152–164
36. Sato, K., Kadiiska, M. B., Ghio, A. J., Corbett, J., Fann, Y. C., Holland, S. M., Thurman, R. G., and Mason, R. P. (2002) *FASEB J.* **16,** 1713–1720
37. Sato, K., Akaike, T., Kohno, M., Ando, M., and Maeda, H. (1992) *J. Biol. Chem.* **267,** 25371–25377
38. Tanaka, K., Tsutsumi, S., Arai, Y., Hoshino, T., Suzuki, K., Takaki, E., Ito, T., Takeuchi, K., Nakai, A., and Mizushima, T. (2007) *Mol. Pharmacol.* **71,** 985–993
39. Asano, T., Tanaka, K., Yamakawa, N., Adachi, H., Sobue, G., Goto, H., Takeuchi, K., and Mizushima, T. (2009) *J. Pharmacol. Exp. Ther.* **330,** 458–467
40. Suemasu, S., Tanaka, K., Namba, T., Ishihara, T., Katsu, T., Fujimoto, M., Adachi, H., Sobue, G., Takeuchi, K., Nakai, A., and Mizushima, T. (2009) *J. Biol. Chem.* **284,** 19705–19715

[4] Yamashita, Y., Hoshino, T., Matsuda, M., Kobayashi, C., Tominaga, A., Nakamura, Y., Nakashima, K., Yokomizo, K., Ikeda, T., Mineda, K., Maji, D., Niwano, Y., and Mizushima, T. (2010) *Exp. Dermatol.*, in press.

41. Hirakawa, T., Rokutan, K., Nikawa, T., and Kishi, K. (1996) *Gastroenterology* **111,** 345–357
42. Takashima, A., and Bergstresser, P. R. (1996) *Photochem. Photobiol.* **63,** 397–400
43. Feldmeyer, L., Keller, M., Niklaus, G., Hohl, D., Werner, S., and Beer, H. D. (2007) *Curr. Biol.* **17,** 1140–1145
44. Namba, T., Tanaka, K., Ito, Y., Ishihara, T., Hoshino, T., Gotoh, T., Endo, M., Sato, K., and Mizushima, T. (2009) *Am. J. Pathol.* **174,** 1786–1798
45. Jana, N. R., Tanaka, M., Wang, G., and Nukina, N. (2000) *Hum. Mol. Genet.* **9,** 2009–2018
46. Ohkawara, T., Nishihira, J., Takeda, H., Miyashita, K., Kato, K., Kato, M., Sugiyama, T., and Asaka, M. (2005) *Scand. J. Gastroenterol.* **40,** 1049–1057
47. Ohkawara, T., Nishihira, J., Takeda, H., Katsurada, T., Kato, K., Yoshiki, T., Sugiyama, T., and Asaka, M. (2006) *Int. J. Mol. Med.* **17,** 229–234
48. Bickers, D. R., and Athar, M. (2006) *J. Invest. Dermatol.* **126,** 2565–2575
49. Kulms, D., Zeise, E., Pöppelmann, B., and Schwarz, T. (2002) *Oncogene* **21,** 5844–5851
50. Zylicz, M., King, F. W., and Wawrzynow, A. (2001) *EMBO J.* **20,** 4634–4638
51. Raj, D., Brash, D. E., and Grossman, D. (2006) *J. Invest. Dermatol.* **126,** 243–257
52. Guo, S., Wharton, W., Moseley, P., and Shi, H. (2007) *Cell Stress Chaperones* **12,** 245–254
53. Jantschitsch, C., and Trautinger, F. (2003) *Photochem. Photobiol. Sci.* **2,** 899–903
54. Zou, Y., Crowley, D. J., and Van Houten, B. (1998) *J. Biol. Chem.* **273,** 12887–12892
55. Ando, H., Kondoh, H., Ichihashi, M., and Hearing, V. J. (2007) *J. Invest. Dermatol.* **127,** 751–761
56. Bustamante, J., Bredeston, L., Malanga, G., and Mordoh, J. (1993) *Pigment. Cell. Res.* **6,** 348–353
57. Tanaka, K., Hasegawa, J., Asamitsu, K., and Okamoto, T. (2005) *J. Pharmacol. Exp. Ther.* **315,** 624–630

Am J Physiol Lung Cell Mol Physiol 298: L348–L360, 2010.
First published December 24, 2009; doi:10.1152/ajplung.00289.2009.

Therapeutic effect of lecithinized superoxide dismutase on bleomycin-induced pulmonary fibrosis

Ken-Ichiro Tanaka,[1] Tomoaki Ishihara,[1] Arata Azuma,[2] Shoji Kudoh,[2] Masahito Ebina,[3] Toshihiro Nukiwa,[3] Yukihiko Sugiyama,[4] Yuichi Tasaka,[1] Takushi Namba,[1] Tsutomu Ishihara,[1] Keizo Sato,[1] Yutaka Mizushima,[5] and Tohru Mizushima[1]

[1]*Graduate School of Medical and Pharmaceutical Sciences, Kumamoto University, Kumamoto;* [2]*Department of Internal Medicine, Division of Respiratory, Infection, and Oncology, Nippon Medical School, Tokyo;* [3]*Department of Respiratory Medicine, Tohoku University Graduate School of Medicine, Sendai;* [4]*Department of Medicine, Jichi Medical University, Tochigi; and* [5]*DDS Institute, The Jikei University School of Medicine, Tokyo, Japan*

Submitted 20 August 2009; accepted in final form 21 December 2009

Tanaka K, Ishihara T, Azuma A, Kudoh S, Ebina M, Nukiwa T, Sugiyama Y, Tasaka Y, Namba T, Ishihara T, Sato K, Mizushima Y, Mizushima T. Therapeutic effect of lecithinized superoxide dismutase on bleomycin-induced pulmonary fibrosis. *Am J Physiol Lung Cell Mol Physiol* 298: L348–L360, 2010. First published December 24, 2009; doi:10.1152/ajplung.00289.2009.—Idiopathic pulmonary fibrosis (IPF) is thought to involve inflammatory infiltration of leukocytes, lung injury induced by reactive oxygen species (ROS), in particular superoxide anion, and fibrosis (collagen deposition). No treatment has been shown to improve definitively the prognosis for IPF patients. Superoxide dismutase (SOD) catalyzes the dismutation of superoxide anion to hydrogen peroxide, which is subsequently detoxified by catalase. Lecithinized SOD (PC-SOD) has overcome clinical limitations of SOD, including low tissue affinity and low stability in plasma. In this study, we examined the effect of PC-SOD on bleomycin-induced pulmonary fibrosis. Severity of the bleomycin-induced fibrosis in mice was assessed by various methods, including determination of hydroxyproline levels in lung tissue. Intravenous administration of PC-SOD suppressed the bleomycin-induced increase in the number of leukocytes in bronchoalveolar lavage fluid. Bleomycin-induced collagen deposition and increased hydroxyproline levels in the lung were also suppressed in animals treated with PC-SOD, suggesting that PC-SOD suppresses bleomycin-induced pulmonary fibrosis. The dose-response profile of PC-SOD was bell-shaped, but concurrent administration of catalase restored the ameliorative effect at high doses of PC-SOD. Intratracheal administration or inhalation of PC-SOD also attenuated the bleomycin-induced inflammatory response and fibrosis. The bell-shaped dose-response profile of PC-SOD was not observed for these routes of administration. We consider that, compared with intravenous administration, inhalation of PC-SOD may be a more therapeutically beneficial route of administration due to the higher safety and quality of life of the patient treated with this drug.

idiopathic pulmonary fibrosis; reactive oxygen species

IDIOPATHIC PULMONARY FIBROSIS (IPF) is a progressive and devastating chronic lung condition with poor prognosis; the mean length of survival from the time of diagnosis is 2.8–4.2 years. IPF progresses insidiously and slowly, and acute exacerbation of IPF is a highly lethal clinical event (1, 4, 21, 36). Current agents for the treatment of IPF, such as steroids and immunosuppressors, have not been found to improve the prognosis (1, 2, 26, 47), thus requiring the development of new types of drugs to treat IPF. To evaluate candidate drugs, the bleomycin-induced pulmonary fibrosis animal model provides a convenient option for the study (33).

Although the etiology of IPF is not yet fully understood, recent studies have suggested that it is triggered by lung injury and inflammation [infiltration of leukocytes (such as alveolar macrophages, lymphocytes, and neutrophils) and activation of cytokines]. Reactive oxygen species (ROS) that are released from the activated leukocytes cause further lung injury and inflammation. On the other hand, ROS and activated cytokines, especially TGF-β1, stimulate abnormal fibrosis (abnormal wound repair and remodeling) that is characterized by collagen deposition (22, 40). TGF-β1 seems to stimulate the production of interstitial collagen through both activation of fibroblasts and transformation of epithelial cells to fibroblasts (epithelial-mesenchymal transition; EMT) (3, 6, 48). This abnormal process of fibrosis is responsible for the pulmonary dysfunction associated with IPF. Supporting this idea, genetic inhibition of neutrophil elastase, of the TGF-β1-dependent signal transduction pathway, or of collagen synthesis was reported to suppress the progress of bleomycin-induced pulmonary fibrosis (5, 9, 14, 52). However, it is not clear whether pharmacological inhibition of these factors can improve the prognosis for IPF in humans.

A number of previous studies have suggested that the cellular redox state, determined by the balance between ROS (such as the superoxide anion) and antioxidant molecules [such as superoxide dismutase (SOD) and glutathione], plays an important role in the pathogenesis of IPF. Pulmonary inflammatory cells prepared from IPF patients generated higher levels of ROS than those from controls (25, 45). An increase in the level of ROS was reported in pulmonary tissues, blood, and bronchoalveolar lavage fluid (BALF) of IPF patients and bleomycin-administered animals (8, 18, 38, 41). Genetic modulation that increases or decreases the pulmonary level of ROS resulted in stimulation or suppression, respectively, of bleomycin-induced pulmonary fibrosis (11, 29). Thus, antioxidant molecules have attracted considerable attention as therapeutic candidates for the treatment of IPF. In fact, administration of *N*-acetylcysteine (NAC), which stimulates the synthesis of glutathione, exhibited therapeutic effects on IPF patients and bleomycin-induced pulmonary fibrosis in animals (10, 30, 31, 39).

SOD catalyzes the dismutation of superoxide anion to hydrogen peroxide, which is subsequently detoxified to oxygen and water by catalase or glutathione peroxidase (23). A decreased level of SOD was observed both in IPF patients and in

Address for reprint requests and other correspondence: T. Mizushima, Graduate School of Medical and Pharmaceutical Sciences, Kumamoto Univ., 5-1 Oe-honmachi, Kumamoto 862-0973, Japan (e-mail: mizu@gpo.kumamoto-u.ac.jp).

animals with bleomycin-induced pulmonary fibrosis (37, 53), thus suggesting that increasing SOD could be of therapeutic benefit in the treatment of IPF. However, the low affinity of SOD to the cell membrane where superoxide anion is produced, and its low stability in plasma, with a half-life of only a few minutes, were obstacles to the application of SOD in a clinical setting (13, 16, 17, 46). As a result of this, various SOD drug delivery systems have been devised to help overcome these limitations (16, 17, 20, 51).

Among these applications, lecithinized SOD (PC-SOD) has potentially beneficial effects for the treatment of IPF. PC-SOD is lecithinized human Cu/Zn-SOD in which four phosphatidylcholine (PC) derivative molecules are covalently bound to each SOD dimer (17). In vitro experiments with cultured cells have shown that this modification drastically improves the cell membrane affinity of SOD without decreasing its activity (16, 17), whereas in vivo experiments have demonstrated that it also greatly improves plasma stability (17). In a phase I clinical study, intravenously administered PC-SOD (40–160 mg) had a terminal half-life of more than 24 h, with good safety and tolerability (7, 42), and recently published results of a phase II clinical study have shown that intravenously administered PC-SOD (40 or 80 mg) significantly improved the symptoms of patients of ulcerative colitis (UC), which also involves ROS-induced tissue damage (43). Furthermore, intravenously administered PC-SOD ameliorated bleomycin-induced pulmonary fibrosis in mouse (44, 50), suggesting that PC-SOD could be effective in the treatment of IPF patients. However, a bell-shaped dose-response profile of PC-SOD has been reported for its ameliorative effect against bleomycin-induced pulmonary fibrosis (44, 50). Furthermore, when considering the quality of life (QOL) of patients, the present clinical protocol of PC-SOD administration (daily intravenous infusion for 4 wk) is expected to be improved. In this study, we provide evidence that the ineffectiveness of higher doses of PC-SOD is due to the accumulation of hydrogen peroxide. Furthermore, based on the results obtained here, we propose that administration of PC-SOD by inhalation is a clinically viable option to improve the QOL of IPF patients treated with this drug.

MATERIALS AND METHODS

Chemicals and animals. Paraformaldehyde, FBS, catalase from bovine liver (1,340 U/mg), an antibody against human Cu/Zn-SOD, 4-(dimethylamino)-benzaldehyde (DMBA), chloramine T, potassium dichromate, phosphotungstic acid, phosphomolybdic acid, Orange G, and acid fuchsin were obtained from Sigma (St. Louis, MO). Bleomycin was from Nippon Kayaku (Tokyo, Japan). Novo-heparin (5,000 units) for injection was from Mochida Pharmaceutical (Tokyo, Japan). Chloral hydrate was from Nacalai Tesque (Kyoto, Japan). Diff-Quik was from Sysmex (Kobe, Japan). Terminal deoxynucleotidyl transferase was obtained from Toyobo (Osaka, Japan). Biotin 14-ATP and Alexa Fluor 488 conjugated with streptavidin were purchased from Invitrogen (Carlsbad, CA). An ELISA kit for TGF-β1 was from R&D Systems (Minneapolis, MN). Mounting medium for immunohistochemical analysis (Vectashield) was from Vector Laboratories (Burlingame, CA). Cytospin 4 was purchased from Thermo Electron, whereas L-hydroxyproline, sodium acetate, TCA, azophloxin, and aniline blue were from Wako Pure Chemicals (Tokyo, Japan). Xylidine ponceau was from Waldeck (Muenster, Germany), and Mayer's hematoxylin, 1% eosin alcohol solution, mounting medium for histological examination (malinol), and Weigert's iron hematoxylin were from Muto Pure Chemicals (Tokyo, Japan). PC-SOD (3,000 U/mg) was from our laboratory stock (17). DAPI was from Dojindo (Kumamoto, Japan). Wild-type mice (6–8 wk old, ICR, male) were used. The experiments and procedures described here were carried out in accordance with the Guide for the Care and Use of Laboratory Animals as adopted and promulgated by the National Institutes of Health, and were approved by the Animal Care Committee of Kumamoto University.

Administration of bleomycin, PC-SOD, and catalase. ICR mice maintained under anesthesia with chloral hydrate (500 mg/kg) were given one intratracheal injection of bleomycin (5 mg/kg) in PBS (1 ml/kg) by use of micropipette (p200) to induce an inflammatory response and fibrosis. PC-SOD and catalase were dissolved in 5% xylitol and administered intravenously (tail vein) or intratracheally. For control mice, 5% xylitol solution was administered. The first administration of PC-SOD was performed just before the bleomycin administration.

For administration of PC-SOD by inhalation, five mice were placed in a chamber (volume, 45 l) and maintained under normoxic and normocapnic conditions. PC-SOD was dissolved in 10 ml of 5% xylitol, and an ultrasonic nebulizer (NE-U17 from Omron, Tokyo, Japan) that was connected to the chamber was used to nebulize the entire volume of the PC-SOD solution in 30 min. For control mice, 5% xylitol solution was subjected to nebulizer. Mice were kept in the chamber for a further 10 min after the 30 min of nebulizing.

Preparation of BALF and cell count. BALF was collected by cannulating the trachea and lavaging the lung with 1 ml of sterile PBS containing 50 U/ml heparin (two times). About 1.8 ml of BALF was routinely recovered from each animal. The total cell number was counted using a hemocytometer. Cells were stained with Diff-Quik reagents, and the ratios of alveolar macrophages, lymphocytes, and neutrophils to total cells were determined. More than 100 cells were counted for each sample.

Histological and immunohistochemical analyses and TUNEL assay. Lung tissue samples were fixed in 4% buffered paraformaldehyde and then embedded in paraffin before being cut into 4-μm-thick sections.

For histological examination, sections were stained first with Mayer's hematoxylin and then with 1% eosin alcohol solution. Samples were mounted with malinol and inspected with the aid of an Olympus BX51 microscope.

For staining of collagen (Masson's trichrome staining), sections were sequentially treated with *solution A* [5% (wt/vol) potassium dichromate and 5% (wt/vol) trichloroacetic acid], Weigert's iron hematoxylin, *solution B* [1.25% (wt/vol) phosphotungstic acid and 1.25% (wt/vol) phosphomolybdic acid], 0.75% (wt/vol) Orange G solution, *solution C* [0.12% (wt/vol) xylidine ponceau, 0.04% (wt/vol) acid fuchsin, and 0.02% (wt/vol) azophloxin], 2.5% (wt/vol) phosphotungstic acid, and finally aniline blue solution. Samples were mounted with malinol and inspected with the aid of an Olympus BX51 microscope.

For immunohistochemical analysis, sections were treated with 20 μg/ml protease K for antigen activation and incubated with 0.3% hydrogen peroxide in methanol for removal of endogenous peroxidase. Sections were blocked with 2.5% goat serum for 10 min, incubated for 12 h with an antibody against human Cu/Zn-SOD (1:200 dilution) in the presence of 2.5% BSA, and then incubated for 1 h with peroxidase-labeled polymer conjugated to goat anti-mouse immunoglobulins. Then, 3, 3′-diaminobenzidine was applied to the sections, and the sections were finally incubated with Mayer's hematoxylin. Samples were mounted with malinol and inspected using a fluorescence microscope (Olympus BX51).

For the TUNEL assay, sections were incubated first with proteinase K (20 μg/ml) for 15 min at 37°C, then with TdTase and biotin 14-ATP for 1 h at 37°C, and finally with Alexa Fluor 488 conjugated with streptavidin and DAPI (5 μg/ml) for 2 h. Samples were mounted with Vectashield and inspected with the aid of a fluorescence microscope (Olympus BX51).

Hydroxyproline determination. Hydroxyproline content was determined as described (49). Briefly, the right lung was removed and homogenized in 0.5 ml of 5% TCA. After centrifugation, pellets were hydrolyzed in 0.5 ml of 10 N HCl for 16 h at 110°C. Each sample was incubated for 20 min at room temperature after addition of 0.5 ml of 1.4% (wt/vol) chloramine T solution and then incubated at 65°C for 10 min after addition of 0.5 ml of Ehrlich's reagent [1 M DMBA, 70% (vol/vol) isopropanol and 30% (vol/vol) perchloric acid]. Absorbance was measured at 550 nm, and the amount of hydroxyproline was determined.

Determination of the amount of PC-SOD, TGF-β1, and hydrogen peroxide in vivo. Determination of the amount of PC-SOD in serum and tissue was carried out as previously described (17). After administration of PC-SOD, the blood was collected, and serum samples were obtained by centrifugation. Furthermore, lungs were dissected, cut into small pieces, homogenized, and centrifuged to obtain the supernatants. The amount of PC-SOD in samples was determined using a human Cu/Zn-SOD ELISA kit (Bender MedSystem, Burlingame, CA). The amount of TGF-β1 in the lung tissue was also measured by ELISA according to the manufacturer's protocol.

For determination of hydrogen peroxide levels, lungs were dissected, cut into small pieces, suspended in PBS, and incubated for 30 min at 4°C with rotation. After centrifugation, the supernatants were applied to the NWLSS NWK-HYP01 assay kit (Northwest Life Science Specialties, Vancouver, WA).

Real-time RT-PCR analysis. Real-time RT-PCR was performed as previously described (32) with some modifications. Total RNA was extracted from pulmonary tissues using an RNeasy kit according to the manufacturer's protocol. Samples (2.5 μg RNA) were reverse-transcribed using a first-strand cDNA synthesis kit. Synthesized cDNA was used in real-time RT-PCR (Chromo 4 Instrument; Bio-Rad Laboratories, Hercules, CA) experiments using iQ SYBR GREEN Supermix and analyzed with Opticon Monitor Software. Specificity was confirmed by electrophoretic analysis of the reaction products and by inclusion of template- or reverse transcriptase-free controls. To normalize the amount of total RNA present in each reaction, actin cDNA was used as an internal standard.

Primers were designed using the Primer3 website. The primers used were (name: forward primer, reverse primer): *collagen type 1*

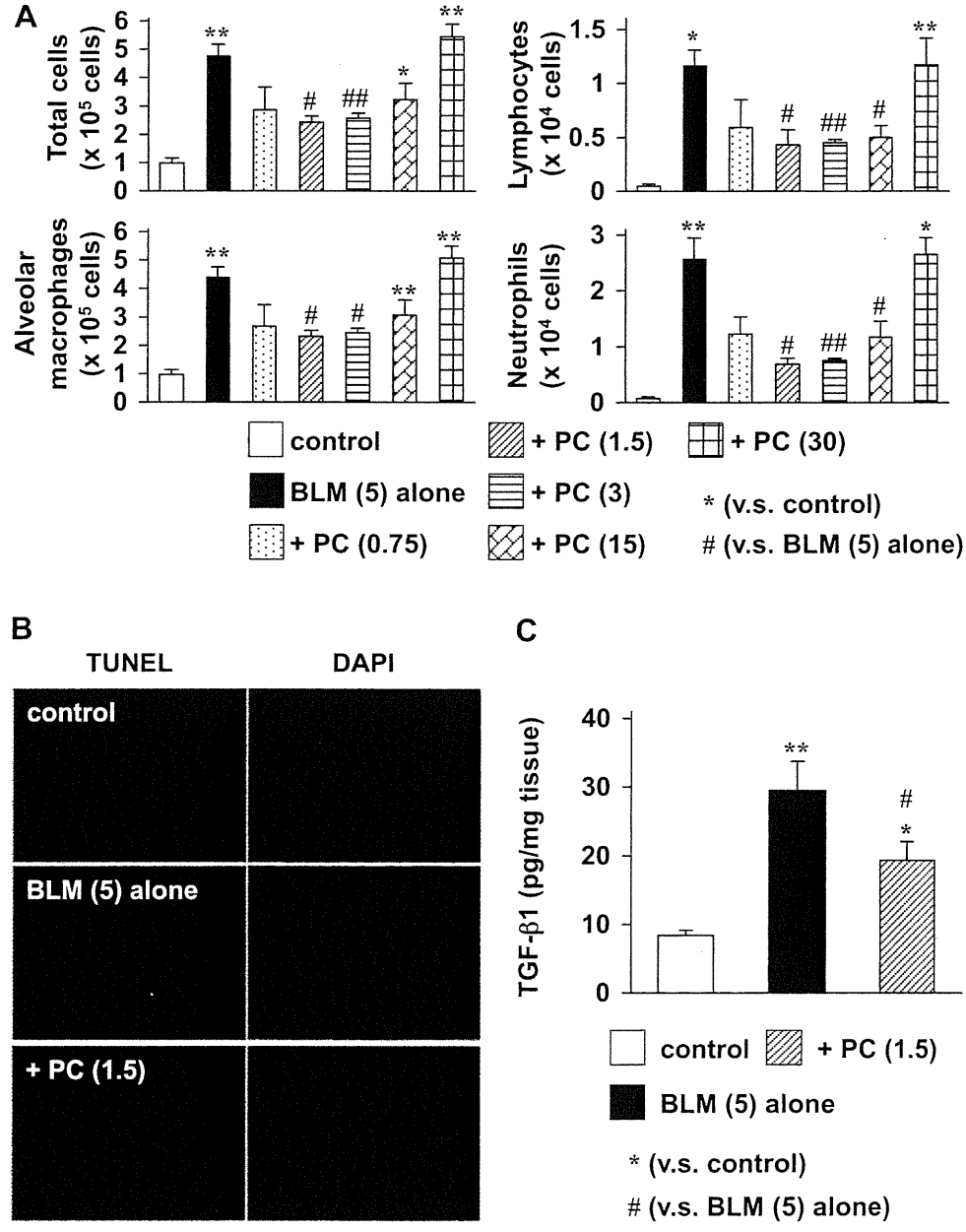

Fig. 1. Effect of intravenous administration of PC-SOD on bleomycin-induced inflammatory response. Mice treated with or without (vehicle) bleomycin (BLM) (5 mg/kg) once-only at *day 0* were intravenously administered indicated doses of PC-SOD (kU/kg) once per day for 3 days (*A–C*). Total cell number and numbers of alveolar macrophages, lymphocytes, and neutrophils were determined after 3 days as described in MATERIALS AND METHODS (*A*). Sections of pulmonary tissue were prepared after 3 days and subjected to TUNEL assay and DAPI staining. Similar results were obtained for at least 3 sections (*B*). The level of TGF-β1 in pulmonary tissue after 3 days was determined by ELISA (*C*). Values are means ± SE. * or #$P < 0.05$; ** or ##$P < 0.01$ (*A* and *C*).

(*Col1a1*): 5′-ccctgtctgcttcctgtaaact-3′, 5′-catgttcggttggtcaaagata-3′; *collagen type 3* (*Col1a3*): 5′-agggcagggaacaacttgatg-3′, 5′-ctccccttttgcacaaagctca-3′; *E-cadherin*: 5′-tgcccagaaaatgaaaaagg-3′, 5′-gtgtatgtggcaatgcgttc-3′; *Actin*: 5′-ggacttcgagcaagagatgg-3′, 5′- agcactgtgttggcgtacag-3′.

Statistical analysis. All values are expressed as means ± SE. Two-way ANOVA followed by the Tukey test or the Student's *t*-test for unpaired results was used to evaluate differences between more than three groups or between two groups, respectively. Differences were considered to be significant for values of $P < 0.05$.

RESULTS

Effect of PC-SOD on bleomycin-induced pulmonary fibrosis. Pulmonary fibrosis was induced in mice given a once-only (at *day 0*) intratracheal administration of bleomycin. The bleomycin-induced inflammatory response can be monitored as a function of the number of inflammatory cells (alveolar macrophages, lymphocytes, and neutrophils) in BALF 3 days after the administration of bleomycin. As shown in Fig. 1*A*, the total number of inflammatory cells and individual numbers of alveolar macrophages, lymphocytes, and neutrophils were all increased by the bleomycin treatment. This effect, however, could be suppressed by the simultaneous intravenous administration of PC-SOD, suggesting that PC-SOD ameliorates the bleomycin-induced pulmonary inflammatory response. PC-SOD produced a maximum beneficial effect at a dosage of 1.5–3 kU/kg, whereas a higher dose (30 kU/kg) did not suppress the bleomycin-induced pulmonary inflammatory response (bell-shaped dose-response profile) (Fig. 1*A*). Administration of the higher dose (30 kU/kg) of PC-SOD alone (without bleomycin administration) did not affect the number of inflammatory cells in BALF (data not shown).

Bleomycin-induced pulmonary fibrosis can be monitored by histopathological analysis and measurement of pulmonary hydroxyproline levels (an indicator of collagen levels) 14 days

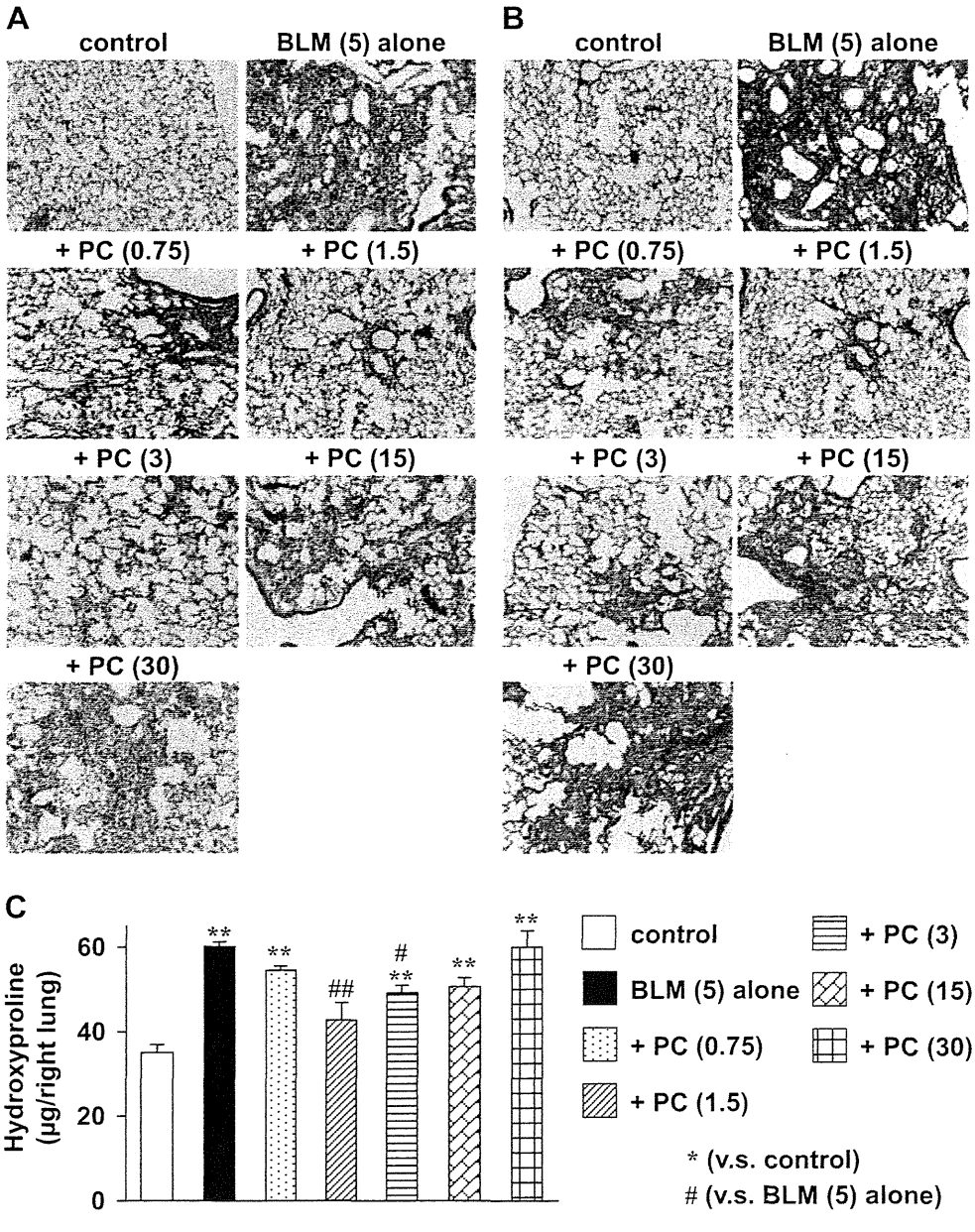

Fig. 2. Effect of intravenous administration of PC-SOD on bleomycin-induced pulmonary fibrosis. Mice treated once-only with or without (control) bleomycin (5 mg/kg) at *day 0* were intravenously administered indicated doses of PC-SOD (kU/kg) once per day for 14 days (*A–C*). Mice treated once-only with bleomycin (5 mg/kg) at *day 0* were intravenously administered indicated doses of PC-SOD (kU/kg) once per day from *day 7* to *day 13* (*D–F*). Sections of pulmonary tissue were prepared after 14 days and subjected to histopathological examination [H&E staining (*A* and *D*) or Masson's trichrome staining (*B* and *E*)] as described in MATERIALS AND METHODS. Similar results were obtained for at least 3 sections (*A*, *B*, *D*, *E*). The pulmonary hydroxyproline level was determined after 14 days as described in MATERIALS AND METHODS. Values are means ± SE. #$P <$ 0.05; ** or ##$P < 0.01$ (*C* and *F*).

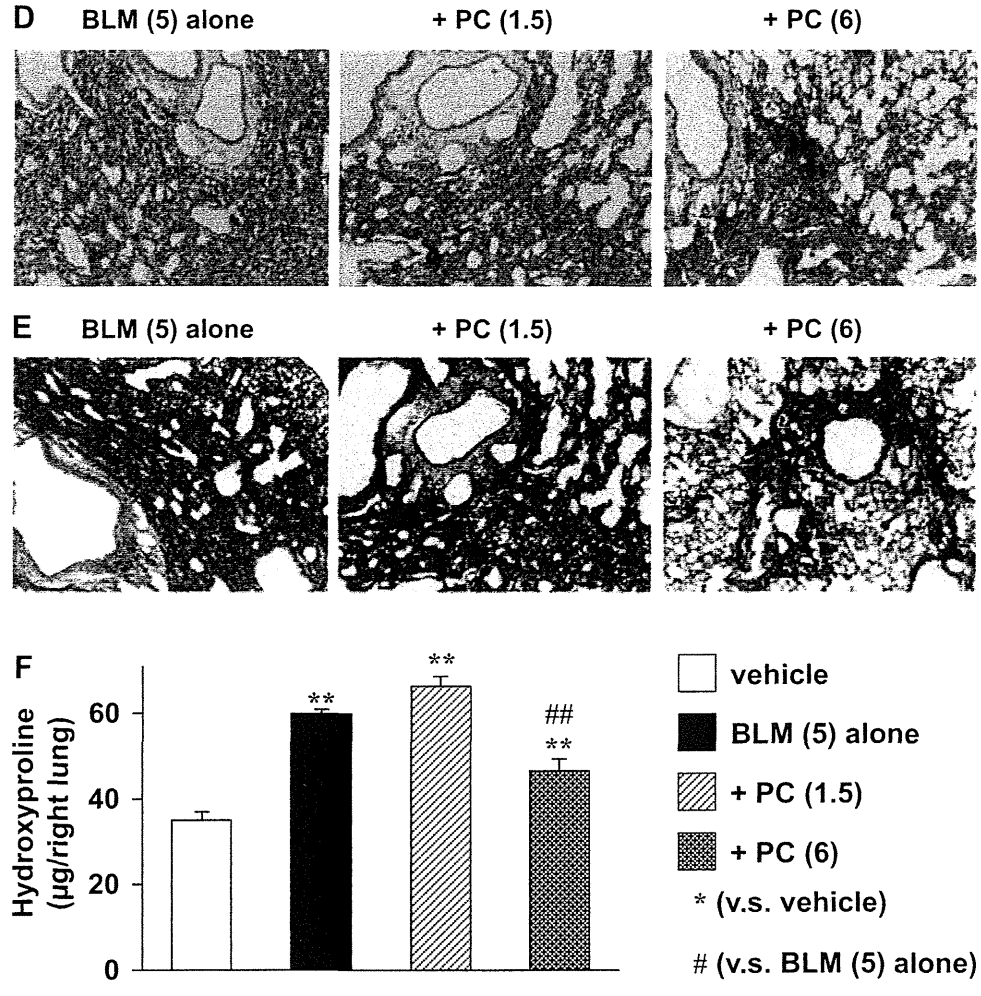

Fig. 2—*Continued*

after the administration of bleomycin. Histopathological analysis of pulmonary tissue using hematoxylin and eosin (H&E) staining revealed that the bleomycin administration induced severe pulmonary damage (thickened and edematous alveolar walls and interstitium) and infiltration of inflammatory cells into these regions (Fig. 2*A*). These phenomena were suppressed by the intravenous administration of PC-SOD (Fig. 2*A*). Again, a bell-shaped dose-response profile was observed; PC-SOD produced a maximum beneficial effect at 1.5–3 kU/kg, whereas at a higher dose (30 kU/kg) this ameliorative effect was not evident (Fig. 2*A*).

Masson's trichrome staining of collagen showed that bleomycin-induced collagen deposition was clearly suppressed by simultaneous intravenous administration of low doses (1.5–3.0 kU/kg) of PC-SOD, but not so clearly for a high dose (30 kU/kg) (Fig. 2*B*). As shown in Fig. 2*C*, a bell-shaped dose-response profile was also observed for the effect of PC-SOD on the bleomycin-induced elevation of pulmonary hydroxyproline content. The results in Fig. 2 thus support the fact that intravenous administration of PC-SOD ameliorates bleomycin-induced pulmonary fibrosis. We used an ELISA assay to determine the level of PC-SOD in serum and pulmonary tissue after its intravenous administration. As shown in Table 1, PC-SOD was detected in serum and pulmonary tissue 6 h after the final injection.

We also examined the effect of intravenous administration of PC-SOD on preexisting fibrosis; intravenous administration of PC-SOD was started at *day 7* after the administration of bleomycin. As shown in Fig. 2, *D–F*, bleomycin-induced

Table 1. *Serum and pulmonary levels of PC-SOD*

PC-SOD, Intravenous, kU/kg	*Plasma, U/ml*	*Lung, mU/mg Tissue*
0.75	7.80 ± 1.38	3.09 ± 0.84
1.5	16.9 ± 0.93	9.06 ± 1.29
15	128 ± 9.5	63.9 ± 1.86
30	245 ± 7.6	109 ± 4.3
PC-SOD, Intratracheal, kU/kg	*Plasma, U/ml*	*Lung, mU/mg Tissue*
0.15	n.d.	20.6 ± 10.5
0.75	0.30 ± 0.03	72.9 ± 5.31
1.5	0.75 ± 0.18	131 ± 28.6
15	5.34 ± 2.58	1,050 ± 381
30	12.5 ± 6.60	2,052 ± 702
60	26.6 ± 7.17	5,412 ± 183
PC-SOD, Inhalation, kU/Chamber	*Plasma, U/ml*	*Lung, mU/mg Tissue*
60	0.12 ± 0.06	22.7 ± 2.97
300	0.36 ± 0.12	51.9 ± 3.66
900	0.57 ± 0.12	198 ± 49.8

Mice treated with or without bleomycin (5 mg/kg) once-only at *day 0* were administered indicated doses of PC-SOD (kU/kg or kU/chamber) intravenously, intratracheally, or by inhalation once daily for 3 days. Blood and pulmonary tissue were taken 6 h after the final administration of PC-SOD. Levels of PC-SOD in samples were determined by ELISA. Values are means ± SE; n.d., not detected.

fibrosis was suppressed by a higher dose of PC-SOD (6 kU/kg) but not its low dose (1.5 kU/kg) under the conditions.

Mechanism for ameliorative effect of PC-SOD on bleomycin-induced pulmonary fibrosis. As described in the introduction, ROS-induced pulmonary cell death and TGF-β1-dependent stimulation of collagen synthesis and EMT play an important role in IPF and bleomycin-induced pulmonary fibrosis (24, 48). We examined effect of intravenous administration of PC-SOD on the extent of pulmonary cell death by employing the TUNEL assay. TUNEL-positive cells (indicative of cell death) increased in response to administration of bleomycin, and this increase was suppressed by simultaneous intravenous administration of PC-SOD (Fig. 1*B*), showing that PC-SOD protects pulmonary cells from cell death in vivo. We also examined the effect of PC-SOD on ROS-induced cell death in vitro, using A549 cells (human alveolar epithelial cell line). As shown in Fig. 3*A*, cell death induced by menadione, a superoxide anion-releasing drug, was inhibited by treatment of cells with PC-SOD.

A bleomycin-induced elevation of TGF-β1 levels in lung tissue was also suppressed by the intravenous administration of PC-SOD (Fig. 1*C*). We then examined effect of PC-SOD on the TGF-β1-dependent induction of collagen expression and EMT in vitro by using real-time RT-PCR analysis. Treatment of HFL-I cells (human embryonic lung fibroblast) with TGF-β1 induced the expression of *Col1a1* and *Col1a3* mRNA; the simultaneous treatment of cells with PC-SOD did not affect this induction (Fig. 3*B*). As shown in Fig. 3*C*, treatment of A549 cells with TGF-β1 induced or suppressed expression of *Col1a1* or *E-cadherin* mRNA, respectively, suggesting that

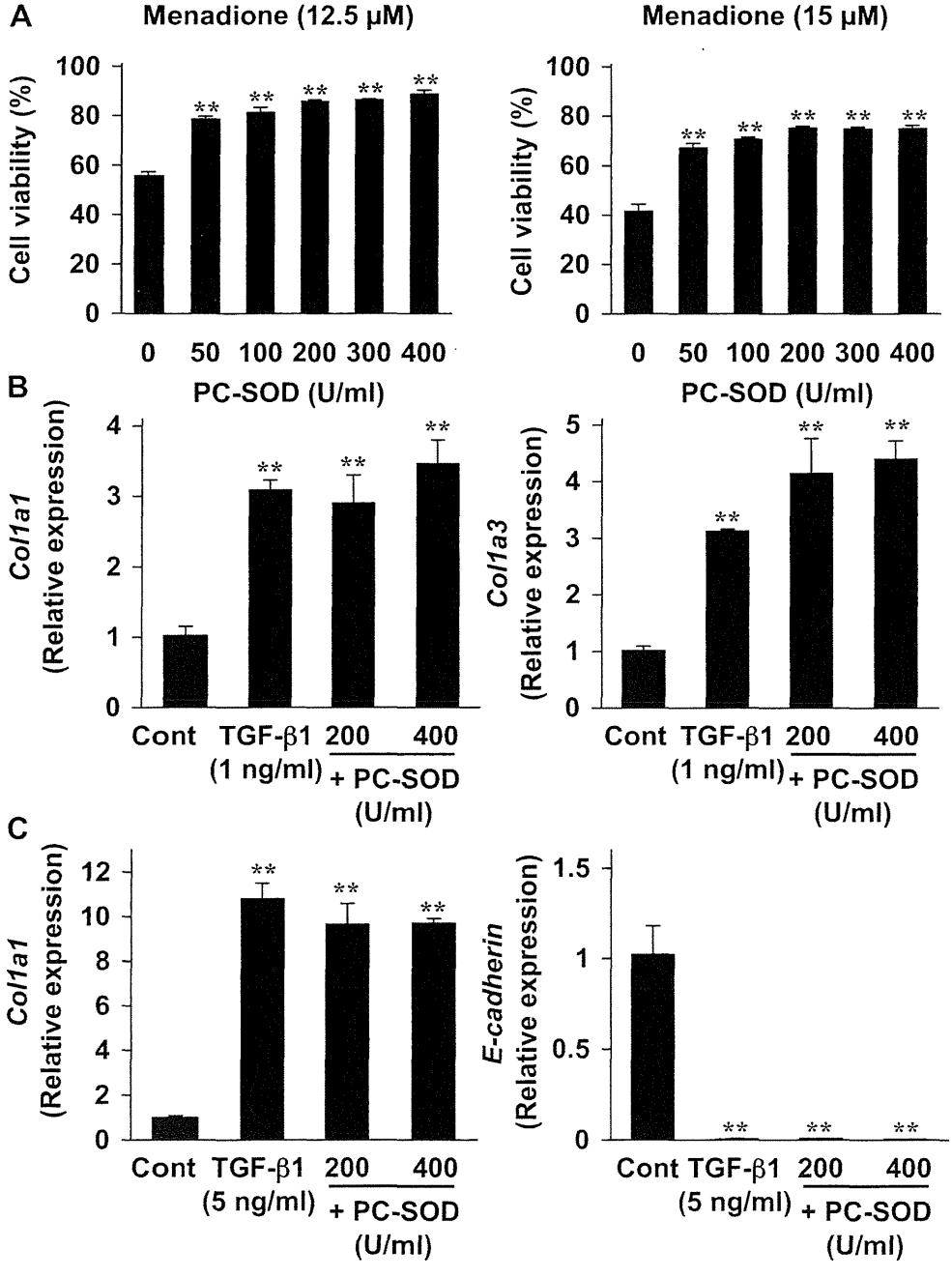

Fig. 3. Effect of PC-SOD on cell death and expression of collagen and epithelial-mesenchymal transition (EMT) in vitro. A549 (*A* and *C*) or HFL-I (*B*) cells were preincubated with the indicated concentration of PC-SOD for 1 h and further incubated with the indicated concentrations of menadione (*A*) or TGF-β1 (*B* and *C*) for 24 h in the presence of the same concentrations of PC-SOD as in the preincubation step. Cell viability was determined by MTT assay (*A*). Total RNA was extracted and subjected to real-time RT-PCR using a specific primer set for each gene. Values were normalized to the actin gene, expressed relative to the control sample (*B* and *C*). Values shown are means ± SE (n = 3). $^{**}P < 0.01$ (*A–C*).

EMT was induced. PC-SOD did not affect these TGF-β1-dependent alterations of mRNA expression (Fig. 3*C*). These results suggest that PC-SOD does not affect the TGF-β1-induced collagen synthesis and EMT.

Effect of simultaneous administration of catalase on the ameliorative effect of PC-SOD against bleomycin-induced pulmonary fibrosis. As described in the introduction, a bell-shaped dose-response profile of PC-SOD against bleomycin-induced pulmonary fibrosis has also been observed in other studies (44, 50). One possible explanation for the ineffectiveness of high doses of PC-SOD to combat the effects of bleomycin is the accumulation of hydrogen peroxide due to the relatively higher activity of SOD compared with catalase. We recently found evidence to support this notion in another animal model; simultaneous administration of catalase restored the ineffectiveness of higher doses of PC-SOD to combat dextran sulfate sodium-induced colitis, an animal model of UC (19). On this basis, we tested here the effect of concurrent administration of catalase on the activity of a high dose of PC-SOD in bleomycin-treated animals. Administration of 30 kU/kg PC-SOD improved the bleomycin-induced inflammatory response (increase in inflammatory cells in BALF) in the presence of the concurrent intravenous administration of catalase (1.5–6 kU/kg), but not in its absence (Fig. 4*A*). Administration of catalase alone did not significantly affect the bleomycin-induced inflammatory response (Fig. 4*A*).

We next examined the effect of simultaneous administration of catalase and high doses of PC-SOD on other aspects of bleomycin-induced pulmonary fibrosis. Bleomycin-induced pulmonary damage and infiltration of inflammatory cells into these regions were clearly suppressed by the simultaneous administration of catalase and a high dose of PC-SOD; however, treatment with either catalase or PC-SOD alone did not bring about such ameliorative effects (Fig. 4*B*). Collagen deposition and an increase in hydroxyproline levels were also clearly suppressed by the simultaneous

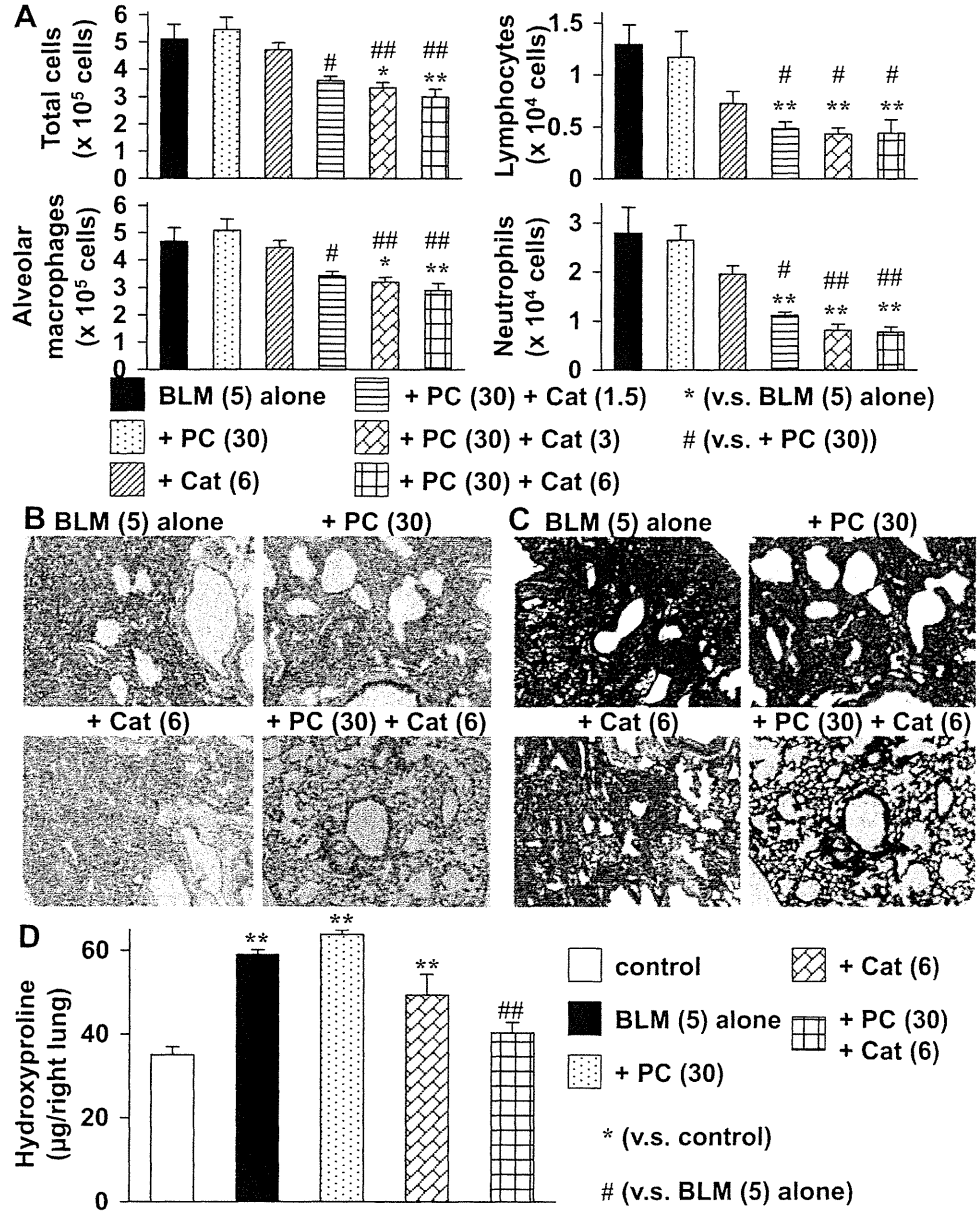

Fig. 4. Effect of concurrent administration of catalase on the ameliorative effect of PC-SOD on the bleomycin-induced inflammatory response and fibrosis. Mice were treated with bleomycin and PC-SOD, and the inflammatory response (*A*) and pulmonary fibrosis (*B–D*) were assessed as described in the legends of Figs. 1 and 2. The indicated dose of catalase (Cat) (kU/kg) was intravenously administered once per day for 3 days (*A*) or 14 days (*B–D*). Similar results were obtained for at least 3 sections (*B* and *C*). Values are means ± SE. * or #$P < 0.05$; ** or ##$P < 0.01$.